Tellus
SERIES B
CHEMICAL
AND PHYSICAL
METEOROLOGY
PUBLISHED BY THE INTERNATIONAL METEOROLOGICAL INSTITUTE IN STOCKHOLM

Tellus (2010), 62B, 455–474

TELLUS

An analysis of the carbon balance of the Arctic Basin from 1997 to 2006

By A. D. McGUIRE[1]*, D. J. HAYES[2], D. W. KICKLIGHTER[3], M. MANIZZA[4,5], Q. ZHUANG[6], M. CHEN[6], M. J. FOLLOWS[4], K. R. GURNEY[6], J. W. McCLELLAND[7], J. M. MELILLO[3], B. J. PETERSON[3] and R. G. PRINN[4] [1]U S Geological Survey, Alaska Cooperative Fish and Wildlife Research Unit, University of Alaska Fairbanks, Fairbanks, AK 99775, USA; [2]Institute of Arctic Biology, University of Alaska Fairbanks, Fairbanks, AK 99775, USA; [3]Marine Biological Laboratory, The Ecosystems Center, Woods Hole, MA 02543, USA; [4]Department of Earth, Atmospheric, and Planetary Sciences, Massachusetts Institute of Technology, Cambridge, MA 02139, USA; [5]Geosciences Research Division, Scripps Institution of Oceanography, University of California San Diego, La Jolla, CA, USA; [6]Department of Earth and Atmospheric Sciences, Purdue University, West Lafayette, IN 47907, USA; [7]Marine Science Institute, University of Texas, Port Aransas, TX 78373, USA

(Manuscript received 27 November 2009; in final form 1 Juy 2010)

ABSTRACT

This study used several model-based tools to analyse the dynamics of the Arctic Basin between 1997 and 2006 as a linked system of land-ocean-atmosphere C exchange. The analysis estimates that terrestrial areas of the Arctic Basin lost 62.9 Tg C yr^{-1} and that the Arctic Ocean gained 94.1 Tg C yr^{-1}. Arctic lands and oceans were a net CO_2 sink of 108.9 Tg C yr^{-1}, which is within the range of uncertainty in estimates from atmospheric inversions. Although both lands and oceans of the Arctic were estimated to be CO_2 sinks, the land sink diminished in strength because of increased fire disturbance compared to previous decades, while the ocean sink increased in strength because of increased biological pump activity associated with reduced sea ice cover. Terrestrial areas of the Arctic were a net source of 41.5 Tg CH_4 yr^{-1} that increased by 0.6 Tg CH_4 yr^{-1} during the decade of analysis, a magnitude that is comparable with an atmospheric inversion of CH_4. Because the radiative forcing of the estimated CH_4 emissions is much greater than the CO_2 sink, the analysis suggests that the Arctic Basin is a substantial net source of green house gas forcing to the climate system.

1. Introduction

Recent studies have revealed surface air temperature increases on the average of 0.6 °C per decade since 1985 over land and ocean areas north of 62°N (Polyakov et al., 2002) and 0.35 °C per decade from 1970 to 2000 for terrestrial regions between 50° and 70°N (Serreze and Francis, 2006; Euskirchen et al., 2007). The recent warming in northern high latitudes is affecting a broad spectrum of physical, ecological and human/cultural systems in this region (Serreze et al., 2000; Chapin et al., 2005; Hinzman et al., 2005; Serreze and Francis, 2006; Post et al., 2009). Some of these changes may be irreversible on century time scales, and have the potential to cause rapid changes in the earth system (Curry et al., 1996; Chapin et al., 2000; McGuire et al., 2006; Lenton et al., 2008). Given the large stores of carbon in northern high latitude regions, the response of the carbon cycle of the Arctic to changes in climate is a major issue of global concern (ACIA, 2004, 2005; McGuire et al., 2006).

While the Arctic is generally considered to play an important role in the global dynamics of both CO_2 and CH_4, there are substantial uncertainties in the magnitude of CO_2 and CH_4 exchange in the Arctic (McGuire et al., 2009). Here we consider the Arctic to encompass the boreal forest biome, the arctic tundra biome, and the Arctic Ocean and its marginal seas. This definition of the Arctic encompasses land and ocean regions from hydrologic (i.e. the Arctic Ocean Basin and lands draining into it) and cryospheric (sea ice and both continuous and discontinuous permafrost) perspectives. Top-down atmospheric analyses indicate that the Arctic is a sink for atmospheric CO_2 of between 0 and 0.8 Pg C yr^{-1} (McGuire et al., 2009), which is between 0 and 25% of the net land/ocean flux of 3.2 Pg C yr^{-1} estimated for the 1990s by the IPCC's 4 th Assessment Report (AR4; Denman et al., 2007). Bottom-up studies estimate (1) that the land sink of the Arctic is between 0.3 and 0.6 Pg C yr^{-1} in the

*Corresponding author.
e-mail: admcguire@alaska.edu
DOI: 10.1111/j.1600-0889.2010.00497.x

late–20th-century (McGuire et al., 2009), which is 30–60% of the 1.0 Pg C yr^{-1} global net land sink estimate for the 1990s, and (2) that the ocean sink of the Arctic is between 24 and 100 Tg yr^{-1}, which is 1–5% of the 2.2 Pg C yr^{-1} net ocean sink estimated globally by AR4 for the same time period (Denman et al., 2007). Atmospheric analyses indicate that the Arctic is a source of CH_4 to the atmosphere of between 15 and 50 Tg CH_4 yr^{-1} (McGuire et al., 2009), which is between 3 and 9% of the net land/ocean source of 552 Tg CH_4 yr^{-1} (582 Tg CH_4 yr^{-1} source–30 Tg CH_4 yr^{-1} soil sink) estimated by AR4 (Denman et al., 2007). In comparison with the top-down analyses, bottom-up analyses indicate that CH_4 emissions have higher lower and upper uncertainty bounds (32 and 112 Tg CH_4 yr^{-1}, respectively) for the net source of CH_4 from the surface to the atmosphere in the Arctic (McGuire et al., 2009). From the global perspective, the transfer of C from land to ocean systems in the Arctic roughly reflects the 11% of global river discharge of water from land to ocean represented by the Pan-Arctic Drainage Basin. Approximately 80 Tg C yr^{-1} as organic and inorganic carbon are transferred from land to ocean via rivers (McGuire et al., 2009), which is approximately 10% of the estimated 0.8 Pg C yr^{-1} transferred from land to ocean via rivers globally (Sarmiento and Gruber, 2006).

Analyses to date indicate that the sensitivity of the carbon cycle of the Arctic during the remainder of the 21st century is also highly uncertain. Observational evidence has identified that a number of features of the Arctic have been substantially changing since the late 1990s including increases in fire (Balshi et al., 2007), decreases in photosynthetic activity (Goetz et al., 2005, 2007), and reductions in sea ice cover (Stroeve et al., 2007). Although we expect that these changes have had consequences for the carbon cycle of the Arctic region, there has not been a comprehensive analysis of how these changes have influenced carbon dynamics in the Arctic. Here we conduct an analysis of the carbon cycle of the Arctic Basin between 1997 and 2006 in which we treat the basin as a linked system of land-based carbon dioxide and methane exchange with the atmosphere, the delivery of land-based dissolved organic carbon to the Arctic Ocean, and the exchange of carbon between the Arctic Ocean and the atmosphere.

2. Methods

2.1. Overview

This study describes an analysis of the contemporary C balance of the Arctic system in which the land and ocean area of the Arctic Basin (Fig. 1a) is treated as a linked system of CO_2 and CH_4 exchange across terrestrial, marine and atmospheric components. The study area for the terrestrial component of the Arctic Basin is defined as the land area within the watersheds of the major rivers that drain into the Arctic Ocean (Lammers et al., 2001). This hydrologic perspective allows the examination of the linkage between the terrestrial and marine components of the Arctic C cycle. The watersheds of the Arctic Basin contain most of the northern high-latitude land underlain with near-surface permafrost (the cryospheric perspective) and encompass large expanses of arctic tundra and boreal forest ecosystems (the

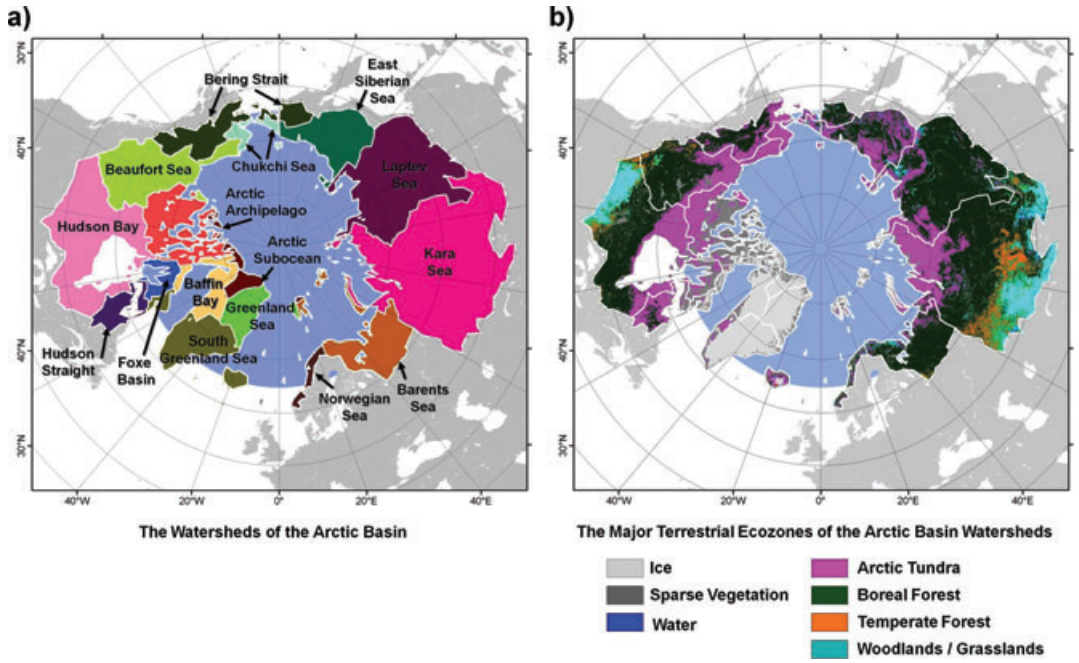

Fig. 1. Maps showing (a) the delineation of the terrestrial watersheds of the Arctic Basin and (b) the spatial distribution of the major ecosystem types across these watersheds.

ecological perspective; Fig. 1b). The marine component of the study includes the area north of 65°N, which covers the whole of the Arctic Ocean proper as well as a portion of its marginal seas.

Several process-based tools were used to conduct this analysis of C dynamics across the Arctic Basin between years 1997 and 2006 through simulations of land–atmosphere CO_2 and CH_4 exchange, the transfer of land-based C to the Arctic Ocean, and ocean–atmosphere CO_2 exchange. CO_2 and CH_4 exchange between the terrestrial ecosystems of the basin and the atmosphere, along with the export of dissolved organic C (DOC) to the Arctic Ocean, were estimated using the Terrestrial Ecosystem Model (TEM), a process-based biogeochemistry model with coupled carbon and nitrogen cycles (Raich et al., 1991). The TEM considers the effects of a number of factors on its simulations of C dynamics including changes in atmospheric CO_2 concentration, tropospheric ozone pollution, nitrogen deposition, climate variability and change and disturbance/land use including fire, forest harvest and agricultural establishment and abandonment. TEM also calculates pyrogenic emissions of CO_2, CH_4 and CO from the combustion of vegetation and soil carbon in wildfires. The DOC leaching dynamics of TEM are a function of soil C decomposition rate, soil DOC concentration and water flux through the soil. We used the methane dynamics module of TEM (MDM-TEM) to estimate the exchange of CH_4 with the atmosphere of both wetlands, which generally emit CH_4 to the atmosphere and uplands, which generally consume CH_4 from the atmosphere. The MDM-TEM considers the effects of a number of factors in its simulations of CH_4 dynamics including the area of wetlands, fluctuations in the water table of wetlands, temperature and labile carbon inputs into the soil solution derived from the net primary production (NPP) estimates of TEM. The MIT ocean biogeochemistry model simulated the net exchange of CO_2 with the atmosphere as driven by changes in sea ice, water temperature, ocean circulation and DOC inputs from TEM.

The results of these simulations were compared with estimates of CO_2 and CH_4 exchange from atmospheric inversion models and with observations of terrestrial C export from Arctic watersheds. The simulated transfer of land-based C to the Arctic Ocean was compared against estimates based on a sampling of DOC export from major Arctic rivers (McClelland et al., 2008). The land–atmosphere CO_2 exchange estimate was compared with results from the TransCom 3 atmospheric inversion model intercomparison project (Gurney et al., 2008), and CH_4 to results from atmospheric inversion-estimated surface emissions (Chen and Prinn, 2006). To compare the 'bottom-up' results from our model simulations with the 'top-down' estimates from these inversion studies, we summarize our estimates of surface-atmosphere CO_2 and CH_4 exchange for the land and ocean area matching the three high-latitude regions defined in the TransCom 3 model experiments (Gurney et al., 2002), namely the Boreal North America, Boreal Asia and Northern Ocean regions.

2.2. *Terrestrial CO_2 fluxes and pyrogenic CH_4 and CO emissions*

We used the TEM as a 'bottom-up' approach to estimate the exchanges of CO_2 with the atmosphere from terrestrial ecosystems of the Arctic Basin. For this study, we used a version of the model (TEM6) that has been modified from Felzer et al. (2004), which simulated ozone pollution effects, to also include the influence of permafrost dynamics (Zhuang et al., 2003; Euskirchen et al., 2006), atmospheric nitrogen deposition, biological nitrogen fixation, DOC leaching, wildfire (Balshi et al., 2007), agricultural conversion and abandonment and timber harvest on terrestrial C dynamics. C pools and associated fluxes are simulated at a monthly time-step for individual 'cohorts' of unique vegetation types and disturbance history organized within spatially explicit 0.5° latitude × 0.5° longitude grid cells. To initialize the C, N and water pools for the beginning of the analysis period (1997–2006), in each model run we simulated dynamics since the year 1000 for each cohort among the 30 169 half-degree grid cells covering the land region north of 45°N. For the Arctic Basin C budget analysis, C fluxes and stock changes are summarized for the basin watersheds (Fig. 1a) and within the Boreal North America and Boreal Asia regions for comparison with the TransCom 3 estimates of land–atmosphere CO_2 flux.

The TEM simulations in this study were driven by temporally- and spatially explicit data sets on atmospheric carbon dioxide concentration ($[CO_2]$), tropospheric ozone (O_3), N deposition, climate variability and change and fire, forest harvest and agricultural establishment and abandonment. Global annual atmospheric $[CO_2]$ data are from the Mauna Loa station (Keeling and Whorf, 2005). $[CO_2]$ data for the time period of years 1000–1900 are held constant at the year 1901 level (296.3 ppm). Monthly air temperature (°C), precipitation (mm) and incident shortwave solar radiation (Wm^{-2}) data derived from observations for the period 1901–2002, gridded at 0.5° resolution, were obtained from the Climate Research Unit (CRU; University of East Anglia, UK; Mitchell and Jones, 2005). The CRU climate variables were extended to 2006 with NCEP/NCAR Reanalysis 1 data sets (NOAA-ESRL Physical Sciences Division, Boulder CO) using a regression procedure based on data anomalies from a 10-yr (1993–2002) mean for each variable (see Drobot et al., 2006). These data sets were hind-casted to year 1000 by a repeating 30-yr cycle of the 1901–1930 monthly data to initialize the carbon pools with climate variability (except for the simulation without climate variability, where 1901–1930 monthly means were used to drive the model for each year). The ozone (O_3) pollution data set used in this study, represented by the AOT40 index (a measure of the accumulated hourly ozone levels above a threshold of 40 ppbv), is based on Felzer et al. (2005) and covers the time period from 1860 to 2006. Before 1860, the ozone level in each 0.5° grid cell was assumed to equal the AOT40 of 1860 (which is equal to zero). The atmospheric N deposition data were based on van Drecht et al. (2003), extended from 2000 to

2006 by adding the difference in annual N deposition rate from 1999 to 2000 to succeeding years, for each 0.5° grid cell [e.g. 2001 N deposition rate = 2000 + (2000–1999), etc.]. For years 1000–1859, annual N deposition was assumed to equal the per grid cell rates in 1860.

The distribution of vegetation types in this study (Fig. 1b; see Table 1) was derived from the Global Land Cover Characterization (GLCC; Loveland et al., 2000) version 2 Seasonal Land Cover Regions (SLCR) data set available at 1km (equal-area) resolution for North America and Eurasia. The translated vegetation map was aggregated to the 0.5° grid matching the input climate data sets while retaining the area represented by each unique vegetation type within a grid cell as an individual, non-spatial cohort. Wetland cohort areas were assigned to each grid cell based on a 1° × 1° grid cell fraction inundated database (Matthews and Fung, 1987), where wetland area equals the product of fraction inundated and total cell area. To enable the evaluation of different disturbance and land use change events, we have developed a number of spatially explicit time series data sets to prescribe the timing, area and distribution of historical disturbances and land use change. Historical annual burn areas for North America from 1950 to 2002 were available from the various Alaska and Canada fire databases compiled for the study by Balshi et al. (2007). That study's fire data sets were extended from 2002 to 2006 with updated data from the U.S. Department of the Interior Bureau of Land Management (Alaska) and the Canadian Large Fire Database. The data were extended for Eurasia using the Global Fire Emission Database version 2 (van der Werf et al., 2006). Forest harvest and land use (crops or pasture) cohorts were created in the input data set, derived from 1° × 1° gridded, annual land use transitions data for years 1700–2000, modelled by Hurtt et al. (2006). For Eurasia, the land use transitions data set was hind-casted to the start of the initialization period by linearly 'ramping-up' the transitions rates from 0% per year (for each 1° × 1° grid cell) starting in year 1000 to the year 1700 rates. For North America, we assumed land use transition rates of 0% prior to the year 1700. For both regions, the data were extended by simply using the 2000 rates for years 2001–2006.

To quantify the effects of the various controlling factors considered in this study on terrestrial C dynamics across the northern high latitude region, we conducted a series of model simulation experiments. A simulation framework was designed to allow an analysis of the relative contribution of the different driving factors to the overall C balance of the system over the recent 10-yr period as compared to the patterns simulated in previous decades. Each simulation builds upon the potential vegetation data set by incorporating an additional transient data set at each successive model run: (1) [CO_2], (2) O_3, (3) N deposition, (4) climate variability, (5) fire, (6) forest harvest and (7) agricultural establishment and abandonment. Since the transient data sets were individually added in each successive run, the effects of each on C flux were determined by subtracting the results of a simulation from those of the subsequent run. In this study, we report the effects of these factors on both terrestrial CO_2 exchange and DOC export.

Information about regional carbon sources and sinks can be derived from a 'top-down' approach based on variations in

Table 1. Summary of areas (Mha = 10^4 km^2) of input land cover and disturbance data for the watersheds draining into Arctic Sea Basins, 1997–2006.

Basin	Total inland	Total upland	Total wetland	Arctic tundra	Boreal forest	Temperate forest	Woodland/ Grassland	Burn	Harvest	Agriculture
0. Outside Basin	1551	1327	118	122	332	413	578	69.11	40.24	295.35
1. Arctic Archipelago	119	70	0	69	1	0	0	0.01	0.00	0.00
2. Arctic Subocean	32	1	0	1	0	0	0	0.00	0.00	0.00
3. Baffin Bay	59	2	0	2	0	0	0	0.00	0.00	0.00
4. Barents Sea	127	96	21	20	67	26	4	0.15	2.03	4.02
5. Beaufort Sea	209	171	22	76	102	13	3	7.06	0.91	3.64
6. Bering Strait	121	100	17	68	47	0	1	8.29	0.12	0.02
7. Chukchi Sea	23	19	3	21	1	0	1	0.08	0.00	0.00
8. East Siberian Sea	134	95	33	91	31	0	5	2.46	0.00	0.01
9. Foxe Basin	27	15	0	15	0	0	0	0.00	0.00	0.00
10. Greenland Sea	59	1	0	1	0	0	0	0.00	0.00	0.00
11. Hudson Bay	324	236	59	88	123	28	56	5.90	1.71	58.10
12. Hudson Strait	46	31	9	32	8	0	0	0.10	0.04	0.00
13. Kara Sea	655	492	136	138	264	61	165	35.56	2.27	31.34
14. Laptev Sea	363	333	19	103	226	2	20	14.65	0.28	1.11
15. Norwegian Sea	13	11	0	6	4	1	1	0.00	0.13	0.26
16. South Greenland	117	13	1	12	1	0	1	0.00	0.00	2.03
Basins total	2429	1686	319	743	875	132	256	74	7	101

observed atmospheric [CO_2] via inverse modeling with atmospheric tracer transport models. The land–atmosphere CO_2 exchange estimated by the TEM for this study was compared with model mean and spread from the results of the TransCom 3 project, an intercomparison of atmospheric CO_2 inversion models that includes an ensemble of transport models and model variants (Gurney et al., 2002, 2008). The fluxes from the two approaches are compared on the basis of the net ecosystem exchange (NEE, see Chapin et al., 2006) for two high-latitude TransCom land regions (Boreal North America and Boreal Asia). NEE, a negative value of which indicates a surface sink, is the net flux that integrates all vertical exchanges of CO_2 between the atmosphere and the land and ocean. The TransCom 3 NEE estimates are based on the ensemble of models run on observation data from the 104-station network (a 1995–2006 monthly time series), with the long-term model mean subtracted from deseasonalized flux estimates to remove the bias in the estimates (see Gurney et al., 2008). The TEM calculates monthly NEE for terrestrial ecosystems as the net difference between photosynthetic uptake and the release of CO_2 through plant respiration, decomposition, the decay of harvested products and the CO_2 emissions associated with biomass burning. Because the TEM estimates total C emissions associated with biomass burning (see Balshi et al., 2007), we partitioned the total emissions into pyrogenic emissions of CO_2, CH_4 and CO. The proportion of flaming versus smoldering emissions were determined using ratios for vegetation (80% flaming : 20% smoldering) and soil (20% : 80%) C converted in fire, based on Kasischke and Bruhwiler (2003). The mean emission factors reported in French et al. (2002) were used to calculate the amount of each gas released in fires. Only the emissions of C as CO_2 are included in the calculation of NEE, while C emitted as CH_4 (f_{CH4}) and CO (f_{CO}) is included in the net ecosystem C balance (NECB; see Chapin et al., 2006). We use the sign conventions for NEE and NECB as defined by Chapin et al. (2006) in which a positive NEE follows the atmospheric sciences sign convention and represents a net flux of CO_2 from the surface to the atmosphere (a terrestrial or marine source of CO_2). In contrast, NECB follows the ecological sciences sign convention in which a positive NECB represents a net sink of C (i.e. accounting for all forms of C including CO_2, CO, CH_4, DOC, etc.) in land or ocean ecosystems. Thus, NEE represents the strength of a CO_2 source or sink from the land surface, while NECB represents the change in total C storage of an ecosystem. NEE from the TransCom 3 estimates and the model estimates of this study are compared monthly, annually and as deseasonalized fluxes, the latter calculated as the 13-month trapezoidal mean on monthly NEE (Gurney et al., 2008).

2.3. *Terrestrial CH_4 fluxes*

We used the MDM-TEM as a 'bottom-up' approach to estimate the biogenic exchanges of CH_4 with the atmosphere from terrestrial ecosystems of the Arctic Basin. The MDM-TEM explicitly simulates the processes of CH_4 production and CH_4 oxidation as well as the transport of the gas between the soil and the atmosphere to estimate net biogenic CH_4 emissions (Zhuang et al., 2004, 2007). The model description and parametrizations for both upland and wetland ecosystems are documented in our previous studies (Zhuang et al., 2004, 2006). To simulate net biogenic CH_4 exchanges in our study area, which is spatially heterogeneous with respect to land ecosystem types, soils and climate, we apply the module to each 0.5° (latitude × longitude) grid cell within the study area. The regional net CH_4 emissions are estimated as the difference between CH_4 emissions from wetland ecosystems and CH_4 consumption in upland ecosystems. The MDM-TEM in this study was driven with the climate (air temperature, precipitation and incident short-wave solar radiation), vegetation, elevation and soil texture data described earlier for the simulations of CO_2 exchange by TEM. The MDM-TEM also used vapour pressure data as input, which were assembled from the CRU data sets and extended to 2006 with NCEP, as described above for the other climate variables used in TEM. Monthly air temperature, precipitation and vapour pressure are interpolated into daily time steps following the method described in Zhuang et al. (2004). MDM-TEM was also driven by spatially explicit data on soil water pH (Carter and Scholes, 2000) and leaf area index (LAI). Monthly LAI for our simulation period is organized following Zhuang et al. (2004) with the existing data for the period 1982–1999 (Myneni et al., 1997, 2001). For the period 2000–2006, monthly LAI data were simulated by TEM. During our simulations, LAI is assumed to remain constant within a month, that is, daily LAI in a particular month is assumed to be the mean monthly value of LAI for that month. The NPP data required for driving MDM-TEM were based on the NPP estimates of TEM, which were aggregated over the cohorts within a grid cell for each month of the simulation.

Similar to CO_2, information of regional CH_4 sources can be derived from a 'top-down' approach based on variations in observed atmospheric CH_4 concentrations via inverse modelling with atmospheric tracer transport models. Using an atmospheric inversion approach, Chen and Prinn (2006) estimated methane surface emissions for different methane regional sources and/or processes between 1996 and 2001. Data from 13 high-frequency and 79 low-frequency CH_4 observing sites were averaged into monthly mean values with associated errors arising from instrumental precision, mismatch error and sampling frequency. Simulated methane mole fractions were generated using the 3-D global chemical transport model (MATCH), driven by NCEP analysed observed meteorology (T62 resolution; Kalnay et al., 1996), which accounts for the impact of synoptic and interannually varying transport on methane observations. Monthly Arctic emissions were estimated separately for the North American and Eurasian sectors and these results are compared with the sum of the pyrogenic and biogenic CH_4 emissions estimated by TEM.

2.4. Terrestrial DOC export

We estimate DOC loading to the river networks of the Arctic Basin by simulating DOC production on land and leaching into rivers in TEM. With this approach, we can examine how climate change and disturbance may affect DOC production and loss from land ecosystems. The production of DOC in TEM is assumed to result from the incomplete decomposition of soil organic matter. As a result, the production of DOC depends upon the same factors that influence decomposition, that is, the amount and quality of soil organic matter, soil temperature and soil moisture (see McGuire et al., 1997). The proportion of DOC produced from decomposition is assumed to vary with vegetation type and is determined from annual NPP estimates of intensively studied field sites and annual DOC export either observed in nearby rivers or estimated from review studies (Table 2). Under equilibrium conditions, NPP would equal decomposition rates and DOC production would equal DOC leaching rates. However, for some ecosystems, no DOC leaching is assumed to occur because no water is transferred between the soil and the river networks at the model calibration site. The TEM assumes DOC is stored in the soil until it is leached from this pool based on the concentration of DOC in soil water and the flux of water from soil to the neighbouring river network. We report the effects of the various controlling factors on DOC from the results of the simulation experiments described in Section 2.2.

For linkage to the ocean biogeochemistry model, we use the watershed boundaries (Fig. 1a) to determine the land areas of the Arctic Basin that contribute DOC to the Arctic Ocean. This boundary covers 24.2 million km^2 of land in which 2276 river systems drain into the Arctic Ocean, Hudson Bay and the northern Bering Sea and is represented by 21 025 grid cells (0.5° latitude × 0.5° longitude). DOC export is estimated for each of watersheds draining into the sixteen sea basins by summing the TEM DOC leaching estimates across the grid cells of the appropriate watersheds associated with the sea basins, which represents a conservative estimate of aquatic freshwater processing of DOC.

To evaluate model performance, we compare DOC export estimated by TEM to those obtained by Manizza et al. (2009) using an empirical approach. Manizza et al. (2009) estimate DOC export from rivers draining into ten sea basins identified by Lammers et al. (2001): (1) Arctic Archipelago, (2) Barents Sea, (3) Beaufort Sea, (4) Bering Strait, (5) Chukchi Sea, (6) East Siberian Sea, (7) Hudson Bay, (8) Hudson Strait, (9) Kara Sea and (10) Laptev Sea. The DOC export into the other six sea basins is assumed to be negligible.

2.5. Ocean CO_2 fluxes

The MIT ocean biogeochemistry model used in this study was driven by an ocean general circulation model (OGCM) of the MIT General Circulation Model (Marshall et al., 1997) that includes a coupled sea-ice model. The model is configured on a 'cubed-sphere' grid in a limited area Arctic domain with open boundaries at ∼55°N in the Atlantic and Pacific sectors. Prescribed boundary conditions for potential temperature, salinity, flow and sea-surface elevation are provided from previous integrations of a global configuration of the same model (Menemenlis et al., 2005). The grid is locally orthogonal and has a variable horizontal resolution with an average spacing of ∼18 km, which allows the model to represent eddies. The mesh resolves major Arctic straits, including many of the channels of the Canadian Archipelago. This configuration of the MIT ocean model has also been used to assess the freshwater budget of the Arctic Ocean (Condron et al., 2009).

The atmospheric state (10-m surface winds, 2-m air temperature, humidity and downward long and short-wave radiation) is taken from the six-hourly datasets of the NCEP reanalysis (Kalnay et al., 1996). Monthly mean estuarine fluxes of fresh water are based on the Arctic Runoff database (Shiklomanov et al., 2000; Lammers et al., 2001).

We couple our Arctic OGCM to a simplified ocean biogeochemistry model, which now explicitly represents the transport and cycling of dissolved inorganic carbon (DIC), total alkalinity, phosphate, dissolved organic phosphorus and dissolved oxygen (Dutkiewicz et al., 2005). We added an explicit representation of riverine DOC, which has a time-varying riverine source based on empirical or TEM estimates, as well as a simple representation of the sink due to microbial respiration of this riverine DOC after it reaches the Arctic Ocean; DOC is not explicitly respired to DIC in the rivers in this implementation. We first developed parametrizations of the seasonal and regional delivery of terriginous DOC to the Arctic basin based on an empirical data set (Manizza et al., 2009). We implemented this source in the context of an Arctic basin configuration of the MIT ocean circulation model. Using this framework, we demonstrated that the modelled sources and transport of DOC from terrestrial sources was sufficient to accurately capture the observed relationships between DOC and salinity in the Arctic Ocean provided that the timescale for respiration of DOC in the oceans is about 10 yr (Manizza et al., 2009). Hence, we couple the marine and terrestrial carbon cycles by explicitly representing the influence of riverine DOC in estimating the air–sea CO_2 fluxes in the Arctic Ocean.

3. Results

3.1. Terrestrial CO_2 fluxes

The TEM estimates a net uptake of 51.1 Tg C yr^{-1} as CO_2 from the atmosphere to the land area of the Arctic Basin over the 1997–2006 time period (Table 3, Fig. 2). This terrestrial sink is the result of a positive uptake of 311 Tg C yr^{-1} by the terrestrial component as net ecosystem production (NEP), the balance between net primary productivity (NPP; 4190 Tg C yr^{-1}) in

Table 2. Determination of the ratio of DOC production to decomposition.

Vegetation type	DOC export (g C m^{-2} yr^{-1})	NPP (g C m^{-2} yr^{-1})	DOC : decomposition
Dwarf shrub arctic tundra/alpine tundra	1.2 (Peterson et al., 1986)	65 (McGuire et al., 1992)	0.0186
Low shrub tundra	2.2 (Peterson et al., 1986)	120 (McGuire et al., 1992)	0.0186
Boreal needleleaf evergreen forest	0.9 (MacLean et al., 1999; Petrone, 2005)	152 (Clein et al., 2002)	0.0060
Boreal needleleaf deciduous forest	5.0 (estimate)	424	0.0118
Boreal broadleaf deciduous forest	0.4 (MacLean et al., 1999; Petrone, 2005)	336	0.0012
Temperate needleleaf evergreen forest	4.3 (Aitkenhead and McDowell, 2000)	600	0.0072
Temperate broadleaf deciduous forest	4.3 (Aitkenhead and McDowell, 2000)	730	0.0059
Xeric woodlands	2.67 (Aitkenhead and McDowell, 2000)	550 (McGuire et al., 1992)	0.0049
Xeric Shrubland	0.0 (No river discharge)	110 (McGuire et al., 1992)	0.0000
Grasslands	0.0 (No river discharge)	200 (McGuire et al., 1992)	0.0000

Table 3. Summary of average annual fluxes of carbon (Tg C yr^{-1}) for the watersheds draining into Arctic Sea Basins, 1997–2006.

Basin	NPP	NEP	Fire C (CO_2)	Prod. decay	NEE	DOC export	Wetland C (CH_4)	Fire C (CH_4)	Fire C (CO)	NECB
Arctic Archipelago	44	3.4	0.0	0.0	−3.4	0.9	0.0	0.0	0.0	2.5
Arctic Subocean	0	0.0	0.0	0.0	0.0	0.0	0.0	0.0	0.0	0.0
Baffin Bay	1	0.0	0.0	0.0	0.0	0.0	0.0	0.0	0.0	0.0
Barents Sea	231	8.2	1.9	1.0	−5.3	1.5	1.1	0.0	0.2	2.6
Beaufort Sea	366	31.4	12.5	0.5	−18.3	2.5	1.4	0.1	2.2	12.2
Bering Strait	148	20.9	31.0	0.1	10.2	1.7	1.8	0.4	6.3	−20.4
Chukchi Sea	16	1.1	0.4	0.0	−0.8	0.4	0.2	0.0	0.1	0.1
East Siberian Sea	143	15.0	11.8	0.0	−3.2	1.9	0.0	0.1	2.4	−1.2
Foxe Basin	9	2.1	0.0	0.0	−2.1	0.1	0.0	0.0	0.0	2.0
Greenland Sea	0	0.0	0.0	0.0	0.0	0.0	0.0	0.0	0.0	0.0
Hudson Bay	703	0.3	9.6	7.5	16.8	4.0	4.7	0.1	1.4	−26.8
Hudson Strait	35	−2.6	0.1	0.0	2.7	0.6	0.9	0.0	0.0	−4.2
Kara Sea	1551	138.2	49.7	3.8	−84.7	12.0	16.9	0.4	8.3	47.0
Laptev Sea	915	93.8	129.5	0.4	36.1	10.2	0.9	1.5	25.7	−74.5
Norwegian Sea	17	−0.4	0.1	0.1	0.6	0.2	0.0	0.0	0.0	−0.8
South Greenland	10	−0.4	0.0	0.0	0.4	0.2	0.6	0.0	0.0	−1.2
Basins Total	4190	311.0	246.5	13.5	−51.1	36.3	28.5	2.6	46.6	−62.9

vegetation and the decomposition of soil organic matter through heterotrophic respiration (HR 3879 Tg C yr^{-1}). However, NEP during this time period was substantially offset by the release of C as CO_2 from fires across the Basin (246.5 Tg C yr^{-1}) and the decomposition of agricultural and forestry products (13.5 Tg C yr^{-1}). More than 74% of the pyrogenic CO_2 emissions is attributed to the combustion of soil C (183 Tg C yr^{-1}), which when added to the 23 Tg C yr^{-1} gain to the soil from the difference between litter inputs from vegetation and HR and to other losses from net biogenic CH_4 emissions and DOC export (see next two sections), results in a net loss of 273 Tg C yr^{-1} from the Arctic Basin soil C pool between 1997 and 2006. The loss of soil C is greater than the net gain in vegetation C simulated in this study (207 Tg C yr^{-1}), resulting in an estimated overall loss of 63 Tg C yr^{-1} in ecosystem C stores in the land area of the Arctic Basin over this time period.

Fire emissions account for much of the variability in sources and sinks among watersheds (Table 3), with emissions exceeding NEP to produce CO_2 sources to the atmosphere from the Laptev (36.1 Tg C yr^{-1}) and Bering Strait (10.2 Tg C yr^{-1}) watersheds. Although it had lower fire emissions, the Hudson Bay watershed also acted as a large CO_2 source (16.8 Tg C yr^{-1}) relative to the other North American watersheds because of the large area devoted to agriculture (58 Mha, Table 1) in the watershed. The HR offsets NPP to produce essentially no NEP during this time period in the Hudson Bay watershed, and the C source from this watershed was contributed nearly equally by fire emissions and product decay. The largest sink activity in the Arctic Basin from 1997 to 2006 was found in the Kara Sea watershed (84.7 Tg C yr^{-1}), despite this watershed having the largest area burned (36 Mha) of any watershed over this time period. The fire emissions per area burned are low in the Kara Sea

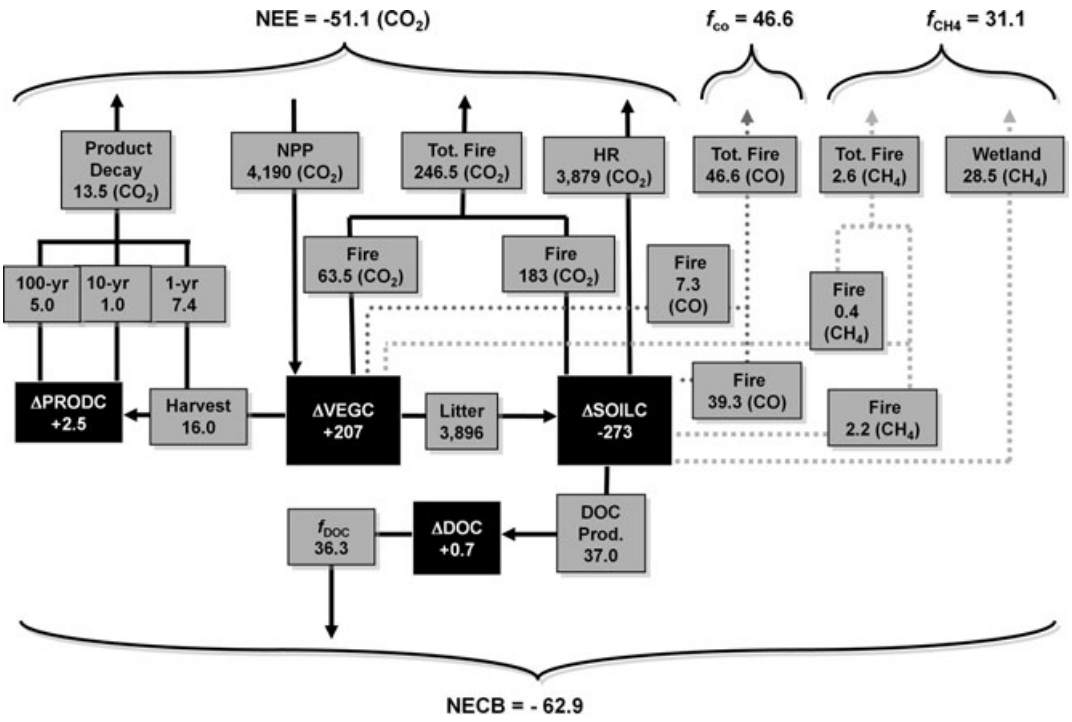

Fig. 2. Simulated carbon stock changes and fluxes (Tg C yr^{-1}) of the terrestrial component of the Arctic Basin, 1997–2006.

watershed because the majority of the burn area between 1997 and 2006 in this watershed (Fig. 3a) occurs in woodland/grassland ecosystems (165 Mha) as well as substantial agricultural areas (31 Mha), which all have a low carbon density. Outside the Kara Sea watershed (compare Figs 1a and 3a), the majority of the burn area from 1997 to 2006 occurred in the boreal forest of the Laptev Sea watershed and across North America, and the major source activity (positive NEE) at the grid cell level (Fig. 3b) corresponds to the pattern of boreal forest fires.

The estimates of land–atmosphere CO_2 exchange in this study are generally consistent with the range of uncertainty in estimates from the atmospheric perspective, although the TEM

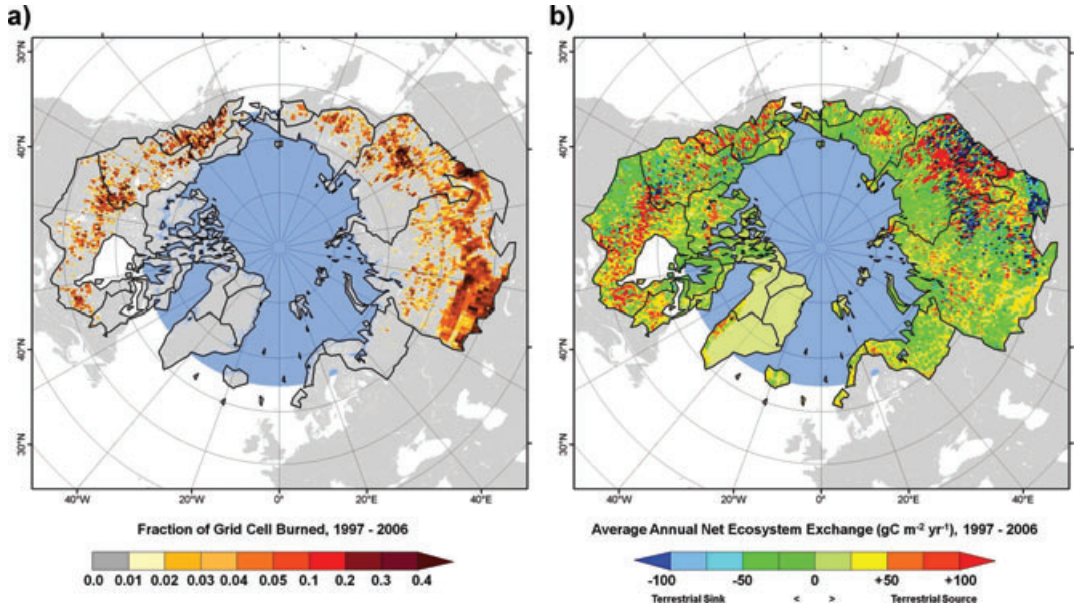

Fig. 3. The spatial pattern of (a) the total fraction of grid cell area burned and (b) the average annual effect (gC m^{-2} yr^{-1}) of all controlling factors on NEE across the watersheds of the Arctic Basin over the 1997–2006 time period.

estimates differ overall in the direction of flux compared to the model means of the TransCom 3 results. The TransCom model means for Boreal North America in the 1995–2006 time frame range from a 60 Tg C yr^{-1} source to a 420 Tg C yr^{-1} sink, depending on the station-data network and the time period bin, with a range of uncertainty of ±31–36 Tg C yr^{-1} around each mean (Gurney et al., 2004; 2008). For the same time period bins between 1995 and 2006, TEM estimates a Boreal North America source of 0–50 Tg C yr^{-1}. For Boreal Asia, TransCom model means suggest a net sink ranging from 30 to 470 Tg C yr^{-1} (±33–48 Tg C yr^{-1}), while TEM estimates of NEE range from –90 to 0 Tg C yr^{-1}, depending on the time period. Monthly NEE estimates from TEM match the seasonal patterns in the TransCom estimates (Figs 4a and b) and are within the range of uncertainty for most months during the 1997–2006 time period. The exceptions occur primarily during the peak draw-down of the summer months, where forward process-based models typically predict lower uptake relative to inverse models (Pacala et al., 2007). The differences in peak uptake between the two estimates are greatest in large fire years when TEM estimates large fire emissions, for example, 2004–2005 in Boreal North America (Fig. 4c) and 2002–2003 in Boreal Asia (Fig. 4d), although the TransCom estimates do show some negative effect on land uptake during those years.

3.2. *Terrestrial CH_4 fluxes*

The combination of the biogenic MDM-TEM and the pyrogenic estimates of CH_4 fluxes indicates that the terrestrial areas of the Arctic Basin annually released approximately 41.5 Tg CH_4 to the atmosphere between 1997 and 2006, with most of the emissions (38.0 Tg CH_4 yr^{-1}) from biogenic sources. These estimates of CH_4 gas emissions translate to 31.1 Tg C–CH_4 yr^{-1} total release, and 28.5 Tg C–CH_4 yr^{-1} from biogenic sources (Table 3), as the molecular weight of carbon is 75% that of methane gas. There is a strong spatial correspondence between CH_4 emissions and the distribution of wetlands in the Arctic Basin (Fig. 5). The Western Siberia Lowland in the Kara Sea watershed and the Hudson Bay Lowland in the Hudson Bay watershed are emission hotspots (Table 3).

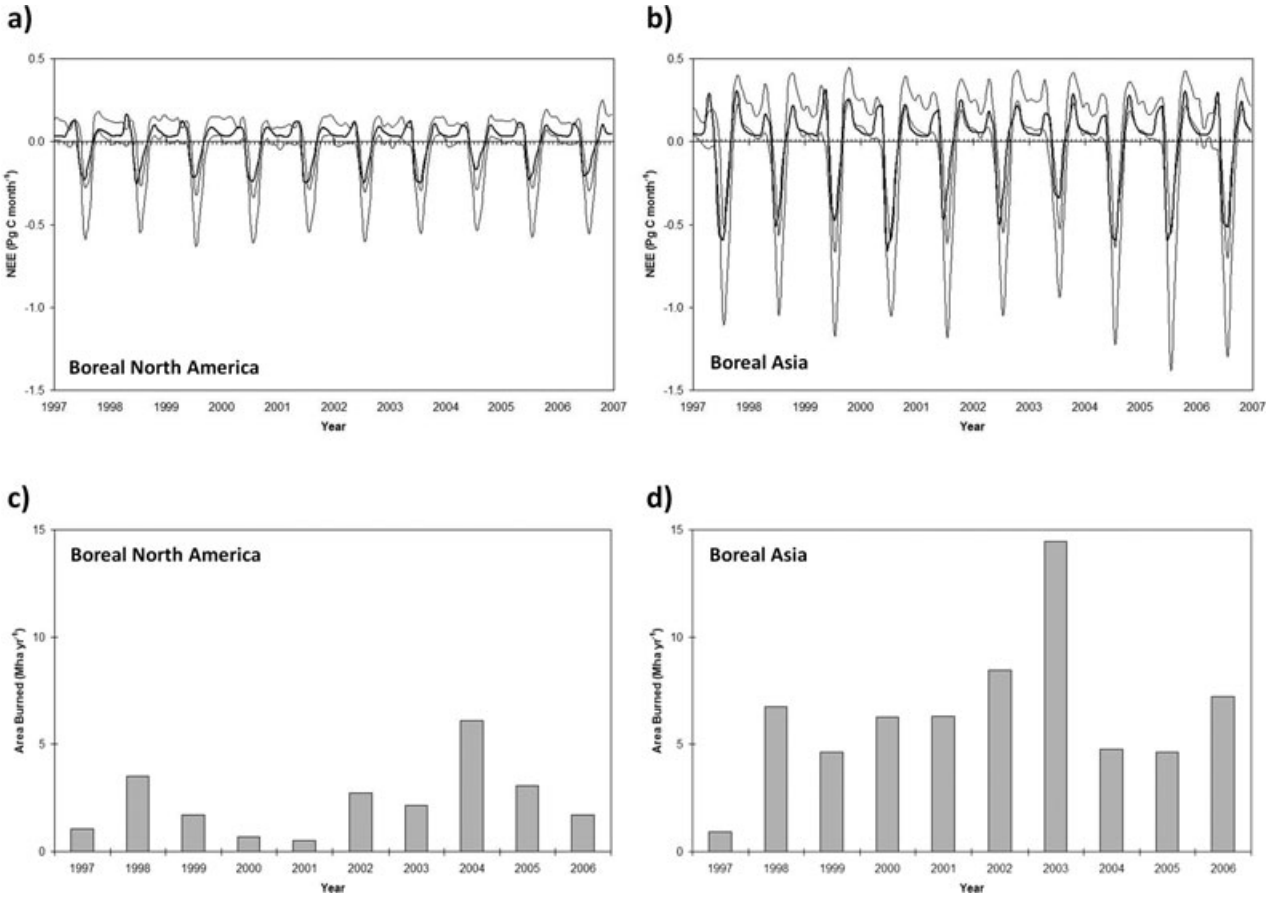

Fig. 4. Comparison of monthly NEE estimates from TEM (thick lines) within the range of uncertainty in TransCom 3 model estimates from the 104 station-data network (thin lines) between 1997 and 2006 for (a) Boreal North America and (b) Boreal Asia. The area burned in (c) Boreal North America and (d) Boreal Asia is also shown for comparison.

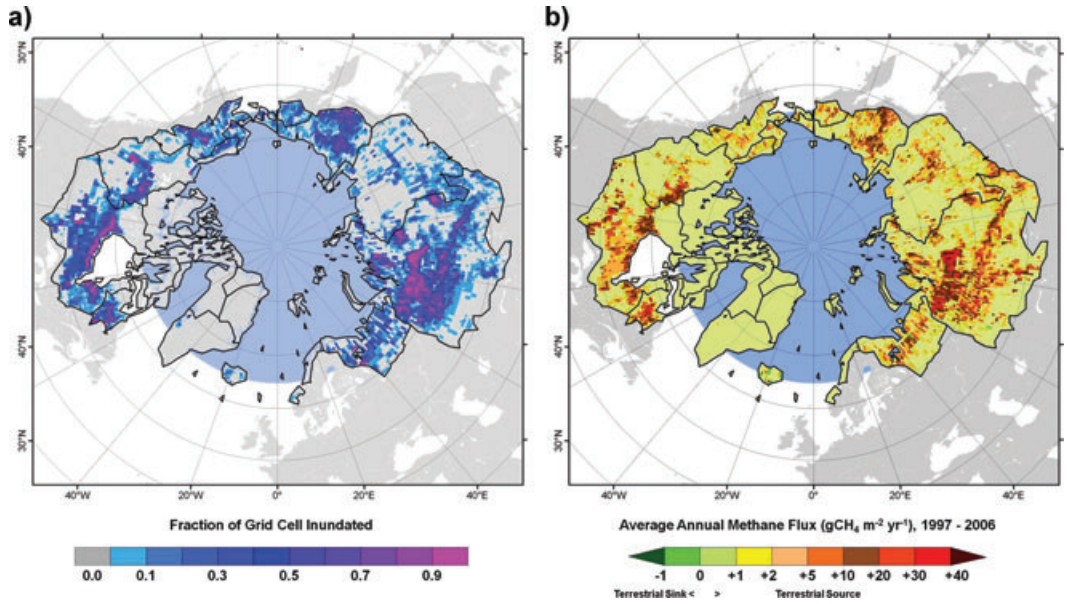

Fig. 5. Spatial patterns of net methane exchange between the terrestrial ecosystems and atmosphere simulated by TEM from 1997 to 2006 (g CH_4 m^{-2} yr^{-1}). Positive values indicate methane emissions from land including both biogenic and pyrogenic CH_4 emissions to the atmosphere and negative values indicate net soil CH_4 consumption.

Our analysis also indicates that the emissions grew on average by 0.6 Tg CH_4 yr^{-1} during the decade of analysis ($R = 0.62$; $n = 11$; $p = 0.04$). There was substantial interannual variation of emissions with the peak emissions in 1998 and lowest emissions in 1997 (Fig. 6). Our simulations indicate that emissions in Boreal Asia increased ($R = 0.66$; slope = 0.6 Tg CH_4 yr^{-1}; $n = 11$; $p = 0.03$), but that emissions in Boreal North America did not change ($R = –0.21$, slope = –0.05 Tg CH_4 yr^{-1}; $n = 11$; $p = 0.50$). Over the decade of analysis, there were very weak trends for increases in air temperature (0.6 °C; $R = 0.33$; $P = 0.3$) and simulated soil temperature (0.14 °C; $R = 0.33$; $p = 0.3$) in Boreal Asia that could have stimulated methanogenesis. While interannual variability in emissions in Boreal Asia was not significantly correlated with changes in soil temperature ($R = 0.25$; $n = 11$; $p = 0.45$), it was marginally correlated with precipitation variability ($R = 0.52$; $n = 11$; $p = 0.09$). Although precipitation seems to control interannual variability in CH_4 emission in Boreal Asia, the increase in simulated water table depth ($R = 0.14$; slope = 0.10 mm yr^{-1}; $p = 0.67$) is weaker than the increases in soil temperature. In contrast, interannual variability of CH_4 emissions in Boreal North America was strongly correlated with interannual variability in air temperature ($R = 0.81$; $n = 11$; $p = 0.002$).

We compared the monthly emissions for 1996–2001 estimated by Chen and Prinn (2006) using a 3D model inverse method for the North American and Eurasian Arctic sectors with the MDM-TEM estimates in Fig. 6. The inversions show well-defined seasonal cycles peaking in July–August with the peak Eurasian emissions being two to three times higher than the North American emissions. The annual average emissions and timing and average amplitudes of the seasonal cycles are in reasonable agreement with the process-based estimates of CH_4 exchange (Fig. 6). The monthly emissions agree well between inversion and process-based modelling estimates in both Boreal Asia ($R = 0.90$; slope = 0.65; $n = 60$; $p < 0.001$) and Boreal North America ($R = 0.89$; slope = 0.88; $n = 60$; $p < 0.001$).

Both our process-based and inversion-based estimates have generally similar standard deviations of CH_4 emissions for the period of 1996–2001, although the variability of CH_4 emissions is somewhat higher for the inversions in North America and somewhat higher for the MDM-TEM in Eurasia. The inversion modeling was conducted on a global scale with prescribed anthropogenic emissions (e.g. coal mining, gas leakage and rice paddy) and other aseasonal natural emissions (e.g. termite, fire emissions) as well as priors of seasonal emissions from wetlands. The interannual variability of wetland emissions in the region is thus determined by those source emissions and global dynamics of atmospheric transport and chemistry. Since the biogenic emissions used in the inversion are different from those of the MDM-TEM estimates, the biogenic emissions from two approaches are independent. The convergence of interannual and seasonal dynamics between two approaches suggests that MDM-TEM estimates of biogenic CH_4 emissions over the region may be accurate for the 1996–2001 time period.

3.3. *Terrestrial DOC export*

The TEM estimates the DOC delivery to the ocean to be 36.3 Tg C yr^{-1} between 1997 and 2006, which is consistent with empirically based estimates of DOC delivery to the ocean

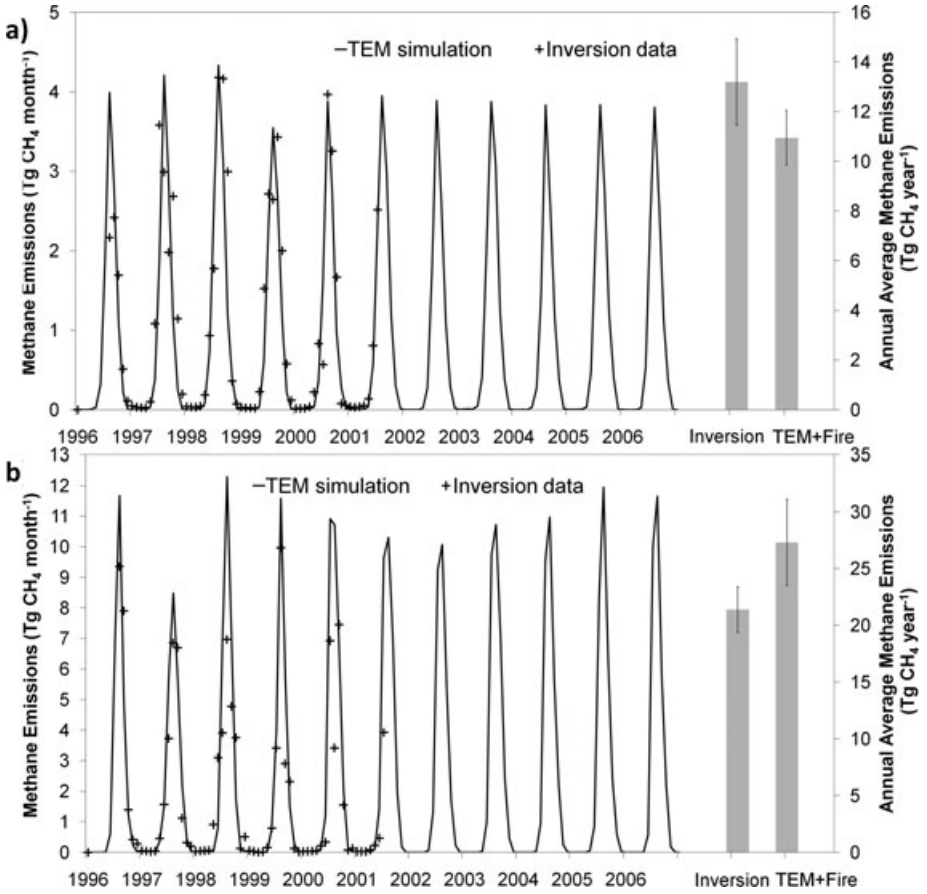

Fig. 6. Comparison CH_4 exchange estimates between TEM and MATCH simulations in (a) Boreal North America and (b) Boreal Asia: Black solid lines show the seasonal dynamics of biogenic and pyrogenic CH_4 emissions estimates of TEM from 1996 to 2006 (Tg CH_4 per month). Black crosses show the seasonal changes of net CH_4 emissions from biogenic and pyrogenic sources from 1996 to 2001 estimated by MATCH (Tg CH_4 per month). Bars show the annual mean for MATCH simulations (1996–2001) and MDM-TEM simulations (1996–2006) as Tg CH_4 yr^{-1}. Error bars indicate standard deviation (interannual variability) for the time period of the inversion simulations (1996–2001).

(Raymond et al., 2007; Manizza et al., 2009). Similar to these other studies, we find that rivers in Eurasia contribute more DOC to the Arctic Ocean (26.3 Tg C yr^{-1}) than rivers in North America (10.0 Tg C yr^{-1}) (Table 3). The Chukchi Sea and Bering Strait receive riverine DOC inputs from both Eurasia and North America (Fig. 1a), but the North American watersheds are estimated to account for almost 80% of the DOC delivered to these sea basins. About a third of the total DOC exported to the Arctic Ocean each year is contributed by rivers emptying into the Kara Sea (Fig. 7; Table 3). Boreal needleleaf deciduous forests and forested wetlands have the largest loss rate of DOC, averaging about 6 g C m^{-2} yr^{-1}, and our analysis suggests that these biomes in the Kara Sea and Laptev Sea watersheds are responsible for over 61% of the terrestrial DOC (22.2 Tg C yr^{-1}) delivered to the Arctic Ocean each year (Fig. 7; Table 3). Between 1997 and 2006 our analysis does not indicate any trend in DOC export.

Overall, the TEM estimate of annual DOC export to the Arctic Ocean (36.3 Tg C yr^{-1}) matches well with the corresponding estimate (37.7 Tg C yr^{-1}) obtained by Manizza et al. (2009). In addition, the TEM estimates for annual DOC export into most of the sea basins are within ±26% of the Manizza et al. (2009) estimates (Fig. 7). However, for a few sea basins (Chukchi Sea, Hudson Strait and Barents Sea), the DOC export estimated by TEM is only 11–35% of the corresponding estimates by Manizza et al. (2009). As the Manizza et al. (2009) DOC export estimates for these three sea basins are based on extrapolation of DOC-discharge relationships developed for watersheds draining into other sea basins, it is not clear how well their estimates represent actual DOC export from these watersheds.

3.4. *Ocean CO_2 fluxes*

Our analysis with the MIT ocean biogeochemistry model estimates that the exchange of CO_2 between the oceanic component of the Arctic Basin and the atmosphere resulted in a net sink of

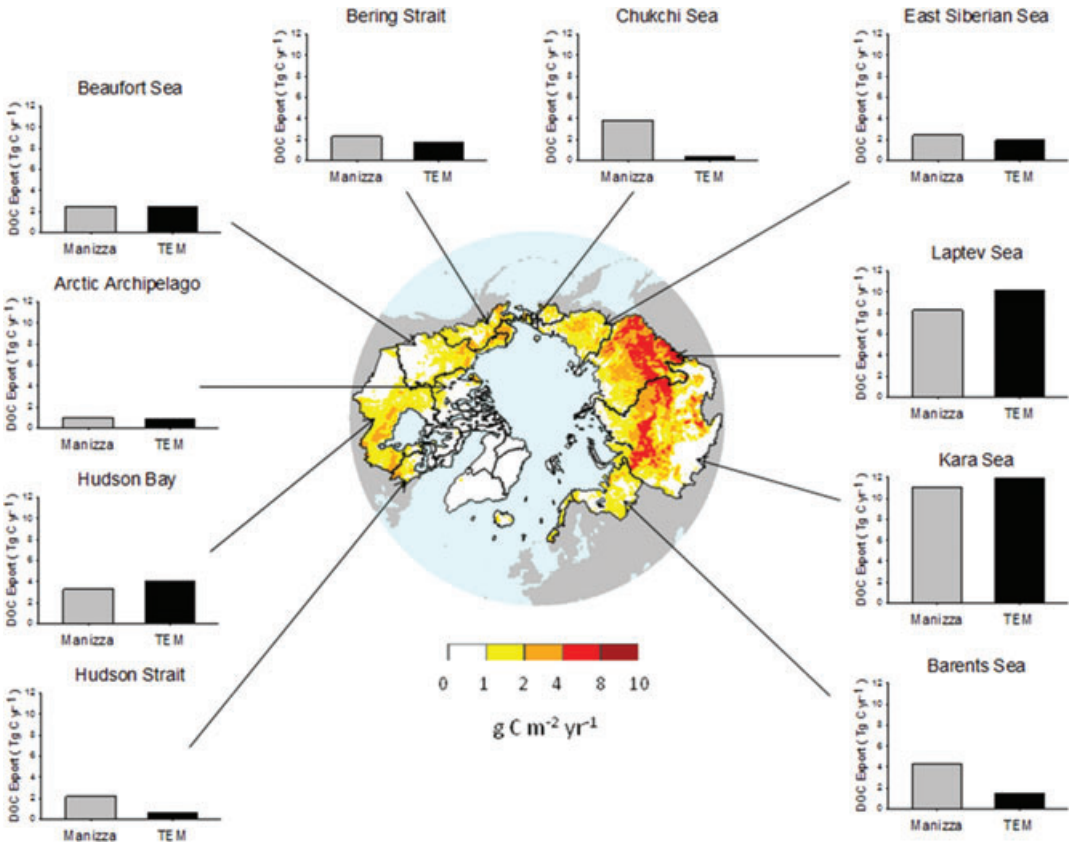

Fig. 7. Mean DOC leaching rates (g C m^{-2} yr^{-1}) estimated by TEM across the Pan-Arctic region and mean DOC export of terrestrial DOC (Tg C yr^{-1}) estimated by Manizza et al. (2009a) and TEM for select watersheds to the Arctic Ocean from 1997 to 2006.

57.8 (±5.5) Tg C yr^{-1} between 1997 and 2006. The time period of 1997–2006 was characterized by substantial changes in sea surface temperature (SST) and sea ice in the Arctic Ocean. The SST estimated by the OGCM in this region shows a clear trend of warming that is mainly due to the increase in the surface air temperature represented in the NCEP re-analysis. The mean SST average in 1997 is –0.47 °C and it increases to –0.11 °C in 2006 (Fig. 8a). In the same area, the progressive warming drives a consequent reduction in sea ice cover (Fig. 8b) that decreases from 10.0 million km^2 in 1996 to 9.4 million km^2 in 2006. As a direct effect, the reduction in sea-ice cover drives an increase in the surface Net Community Production (NCP, the net rate of production in the surface waters accounting for local heterotrophy) in the MIT ocean biogeochemistry model, which is a measure of the local efficiency of the model biological pump. Surface NCP increases from 14.5 Kg C yr^{-1} in 1997 to 17.0 Kg C yr^{-1} in 2006 (Fig. 8d).

In this study, we conducted two simulations to evaluate the effect of different riverine DOC inputs on the regional oceanic CO_2 sink. The first simulations used riverine DOC flux estimated by TEM, (dashed line in Fig. 8c). The second simulation (solid line in Fig. 8c) used a climatological riverine DOC flux that neglects interannual variability of DOC inputs and is based on the combination of modelled freshwater runoff (Lammers et al., 2001) and observed DOC concentrations in Arctic rivers. In both simulations, the CO_2 sink in the Arctic Ocean shows a complex pattern of change with interannual fluctuations driven by climate variability of the re-analysed atmospheric forcing. Overall, the CO_2 sink increases in both simulations (e.g. from ∼54 in 1997 to ∼67 Tg C yr^{-1} in 2006 in the TEM-based simulation; dashed line in Fig. 8c). It appears that the ocean biogeochemical model responds to the substantial reduction of sea-ice cover occurring in 2005 (Figs 8b and c).

The oceanic CO_2 sinks estimated in the two simulations, which are responding to identical forcing in the physical ocean, sea-ice and atmosphere, are characterized by similar temporal variability. However, the CO_2 sink of the simulation using the TEM riverine DOC flux is slightly higher than that of the simulation using the climatological DOC flux. The slightly smaller riverine inputs of DOC from TEM (36.3 versus 37.7 Tg C yr^{-1}) leads to a greater net CO_2 uptake by the Arctic Ocean than in the simulation with the climatological DOC inputs because of less DIC production from HR associated with riverine-derived DOC.

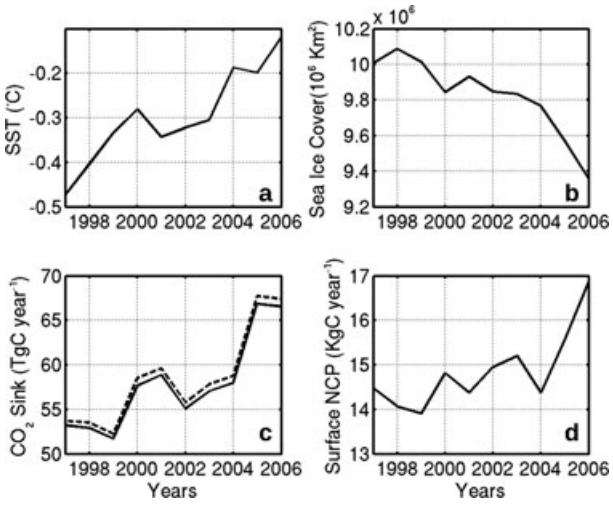

Fig. 8. Annual mean (a) sea surface temperature, (b) sea-ice covered area, (c) CO_2 oceanic sink (solid line is for climatological DOC inputs and dashed line is for TEM DOC inputs) and (d) surface net community production (NCP) for the simulated period 1997–2006. Values are for the oceanic area north of 65°N.

4. Discussion

4.1. Arctic basin carbon budget 1997–2006 and implications for climate forcing

Our analysis indicates that from 1997 to 2006 the terrestrial areas of the Arctic Basin annually gained 51.1 Tg C as CO_2 from the atmosphere, lost 36.3 Tg C as DOC to the ocean, lost 31.1 Tg C as CH_4 and lost 46.6 Tg C as CO to the atmosphere for a total negative carbon balance of 62.9 Tg C yr^{-1} (Table 3; Fig. 9). In contrast, our analysis indicates that the Arctic Ocean took up 57.8 Tg C yr^{-1} as CO_2 from the atmosphere and received 36.3 Tg C yr^{-1} as DOC from the terrestrial component of the Arctic Basin for a total positive carbon balance of 94.1 Tg C yr^{-1}. Overall, our analysis indicates that the Arctic Basin gained 31.2 Tg C yr^{-1} from 1997 to 2006. Our simulations indicate that lands and oceans in the Arctic were a net sink of 108.9 Tg C yr^{-1} CO_2 between 1997 and 2006, which is generally consistent within the range of uncertainty in estimates from the atmospheric perspective (Fig. 10), although the process-based estimates indicate a smaller sink than the model means of the TransCom 3 results because of lower estimated net CO_2 uptake at the peak of the growing season.

Although the Arctic Basin is estimated to be a sink for C, it can generally be considered as a source for greenhouse gas forcing based on the conversion of net CH_4 emissions to CO_2 equivalents. Between 1997 and 2006 our simulations estimate that the region was a net source of 41.5 Tg CH_4 yr^{-1} (31.1 Tg C–CH_4 yr^{-1}), a magnitude that is comparable with the atmospheric inversion of CH_4 we presented in this study and within the uncertainty of other CH_4 inversions (McGuire et al., 2009). This magnitude of CH_4 emissions is equivalent to 1037.5 Tg CO_2 yr^{-1} calculated on a 100-yr time horizon for which one g of CH_4 is equivalent to 25 g of CO_2 in terms of global warming potential (IPCC, 2007). This is nearly 640 Tg CO_2 greater than the net CO_2 sink of 399.3 Tg CO_2 yr^{-1} (108.9 Tg C–CO_2 yr^{-1}) estimated by our simulations. A key issue is whether the global warming potential of the Arctic Basin is evolving to be a greater sink or source of greenhouse gases. To evaluate this issue, we first discuss what our simulations suggest for changes in terrestrial CO_2 exchange and CH_4 exchange with the atmosphere, the delivery of DOC to the ocean and ocean exchange of CO_2 with the atmosphere.

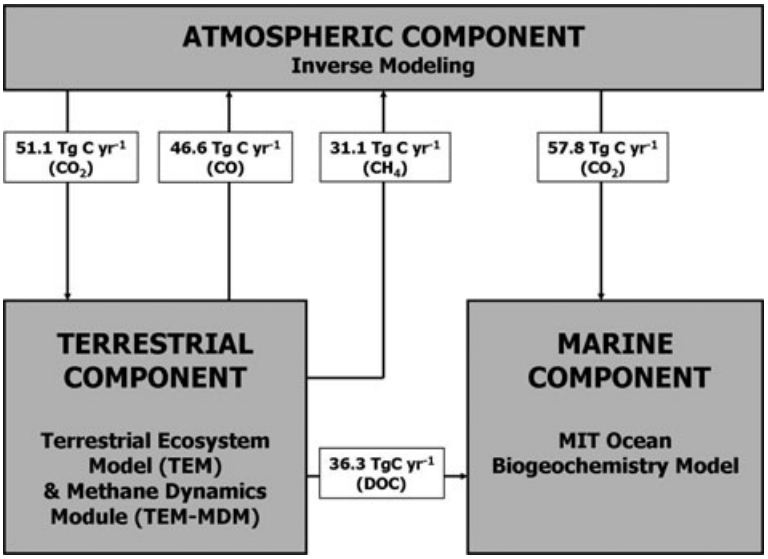

Fig. 9. Overview of the results from this modelling study estimating the fluxes of C as CO_2, CH_4, of CO between the main components of the Arctic Basin system over the 1997–2006 time period.

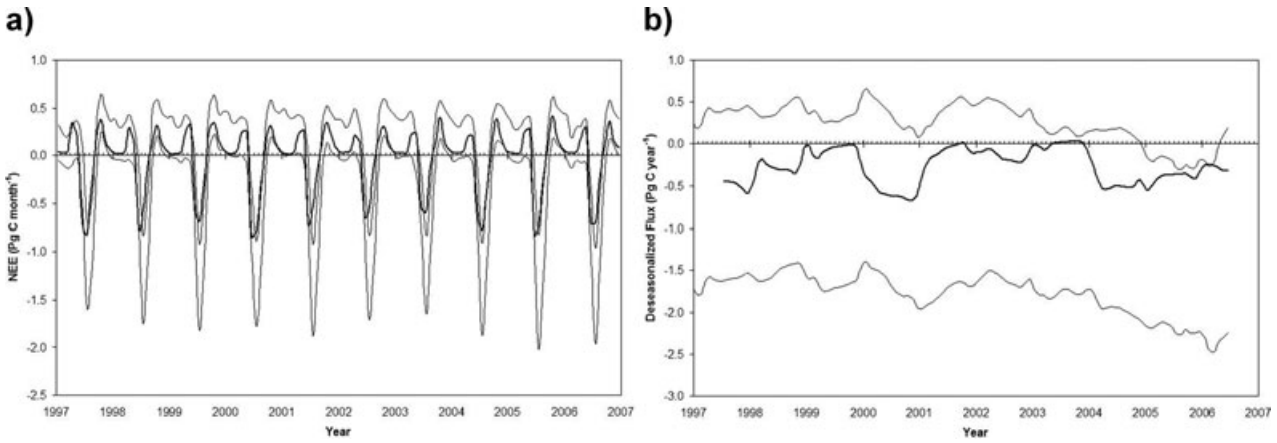

Fig. 10. Comparison of (a) monthly CO_2 flux (Pg C per month) and (b) deseasonalized fluxes (Pg C yr^{-1}) based on the combined land and ocean NEE estimates from the model results of this study (thick lines) within the range of uncertainty in TransCom 3 model estimates from the 104 station-data network (thin lines) aggregated for the Boreal North America, Boreal Asia and Northern Ocean regions, over the 1997–2006 time period.

4.2. Sensitivity of terrestrial CO_2 fluxes

The net uptake of atmospheric CO_2 simulated for the terrestrial ecosystems of the Arctic Basin between 1997 and 2006 is a result of the net uptake in vegetation C through NPP being greater than the release of vegetation C to the atmosphere through fire and harvest and the release of soil C through decomposition and pyrogenic CO_2 emissions (Fig. 2). The net increase in vegetation C is primarily associated with the positive effects of CO_2 fertilization, N deposition and climate (e.g. effects of longer and warmer growing seasons on NPP). The net release of soil C to the atmosphere is a function of warming on decomposition and the combustion of C in more frequent fires. Although not part of NEE, any effect of climate variability that increases biogenic emissions of CH_4 and the leaching of DOC can also contribute to a decrease in the soil C pool. To understand how the effects of these various controlling factors interact to produce the contemporary (1997–2006) dynamics of land–atmosphere CO_2 exchange, it is necessary to compare the importance of the various factors influencing terrestrial CO_2 exchange between the analysis period of this study to previous decades when various studies have suggested that high-latitude terrestrial ecosystems acted as a stronger CO_2 sink (McGuire et al., 2009).

The historical simulations of the C balance of the Arctic Basin using TEM (Fig. 11) indicate a weakening atmospheric CO_2 sink in tundra ecosystems, and a strengthening source from boreal forest ecosystems. The results suggest that CO_2 fertilization effects on NPP are playing the primary role in the C uptake component for both tundra and boreal forest ecosystems, and that these effects are increasing along with the rise in atmospheric [CO_2] over the past several decades. The effect of CO_2 fertilization in our simulations is constrained by N dynamics in the model (McGuire et al., 1997; Kicklighter et al., 1999; Sokolov et al., 2008), particularly in northern high-latitude regions, and is generally less in magnitude than estimated by other global process-based models (McGuire et al., 2001). The consideration of the effects of N limitation on C uptake, as with this study, tends to attenuate ecosystem responses and produce smaller sink estimates (Thornton et al., 2007; Jain et al., 2009) even though the carbon–nitrogen interactions simulated by TEM also allow vegetation uptake of CO_2 to respond positively to enhanced nitrogen availability caused either by additional inputs from atmospheric nitrogen deposition or warming-induced nitrogen mineralization (McGuire et al., 1992; Xiao et al., 1997; Sokolov et al., 2008). Other studies have also shown that CO_2 fertilization effects can play a significant role in the C sink of high-latitude regions (Beer et al., 2006; Balshi et al., 2007), but our results suggest that these effects are largely offset by the source effects of climate and disturbance in the last decade of analysis.

The effect of CO_2 fertilization on NEE has been dampened in tundra ecosystems with an increasing source effect from changes in climate since the 1980s. The source effect of climate variability in tundra ecosystems suggests that increases in decomposition are outpacing any warming-driven increases in NPP to result in a weakening sink. The increases in decomposition in our simulations are a function of greater microbial activity in response to warmer temperatures, as well as a result of more soil C available for decomposition from increasing active layer depths due to permafrost degradation. Other studies suggest that the microbial decomposition of previously frozen organic matter can overcome uptake from increased vegetation productivity to alter the C balance in tundra ecosystems over decadal timescales (Schuur et al., 2009). The simulations show a net C sink in the boreal forest ecosystems of the Arctic Basin prior to the 1980s that has been trending toward an increasing source since the 1980s as a result of climate and disturbance effects. In the last decade of analysis, it is the large positive (source) effect on NEE from fire that is driving the net C source from boreal forests.

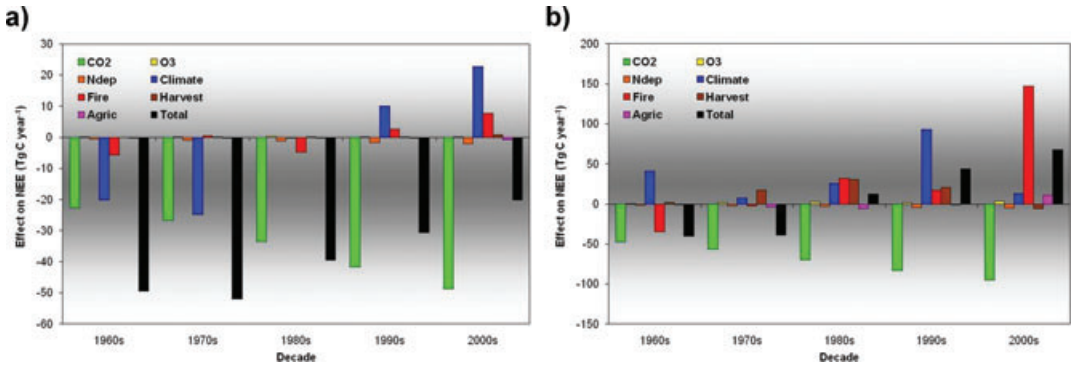

Fig. 11. Total and individual average annual effects (Tg C yr^{-1}) of temporal variability in atmospheric [CO_2], tropospheric O_3 levels, N deposition rates, climate, fire, forest harvest and agricultural establishment and abandonment on NEE for each decade since the 1960s across the Boreal Land Regions in (a) arctic tundra and (b) boreal forest ecosystems.

4.3. Sensitivity of terrestrial CH_4 fluxes

Similar to our previous findings that the regional net CH_4 emissions have increased during the 20th century (Zhuang et al., 2004), our simulation indicates that emissions continued to increase 0.6 Tg CH_4 yr^{-1} between 1996 and 2006. Boreal Asia dominates the trend of increasing emissions while Boreal North America shows no change in emissions. While precipitation seems to control interannual variability in CH_4 emission on Boreal Asia, the increase in simulated water table depth is weaker than the increases in soil temperature over the decade. Estimates of CH_4 emissions by the MDM-TEM are very sensitive to increases in soil temperature, which increase methanogenesis, and changes in water table position, which affect the amount of soil carbon subject to methanogenesis—an anaerobic process (Zhuang et al., 2007). Thus, the slight regional increase of CH_4 emissions appears mainly due to the increasing soil temperature.

A previous analysis with MDM-TEM suggests that climate change has the potential to substantially increase biogenic CH_4 emissions throughout the Arctic Basin during the 21st century (Zhuang et al., 2006). Another analysis focused on Alaska indicates that methane emissions can potentially double by year 2100 and that the temperature sensitivity of methanogenesis dominates over the water table sensitivity (Zhuang et al., 2007), a result that is similar to that of Gedney et al. (2004). We also expect pyrogenic CH_4 emissions to increase with climate change if fire becomes more frequent in northern high latitudes as projected by several studies (Flannigan et al., 1998; Balshi et al., 2009). However, the absolute increase in pyrogenic CH_4 emissions is likely to be small compared to changes in biogenic emissions.

4.4. Sensitivity of terrestrial DOC fluxes

Although no trends in DOC export occur during the 1997–2006 study period, our simulations indicate that DOC delivery to the ocean has been increasing by 0.047 Tg C yr^{-1} over the 20th century (Fig. 12). Based on our factorial simulation experiment, most of this increase (0.039 Tg C yr^{-1}) has been the result of climate variability and change although changes in areas devoted to agriculture and timber harvest have also caused DOC export from this region to increase by 0.010 and 0.002 Tg C yr^{-1}, respectively. In contrast, changes in the fire regime have caused DOC export to decrease by 0.003 Tg C yr^{-1} over the 20th century. Changes in atmospheric chemistry (CO_2, ozone and N deposition) have had rather negligible effects on DOC export over this historical time period.

The response of DOC export to climate variability and change is primarily a result of changes in decomposition rates over this time period whereas the response to land-use change and fire is primarily caused by changes in the availability of the soil organic carbon substrate. As described earlier, warming increases decomposition to enhance the production of DOC from soil organic matter and the amount of DOC available for leaching to the neighbouring river networks. Warmer temperatures also increase the active layer depth due to permafrost degradation to influence DOC export. This exposes more soil organic matter to

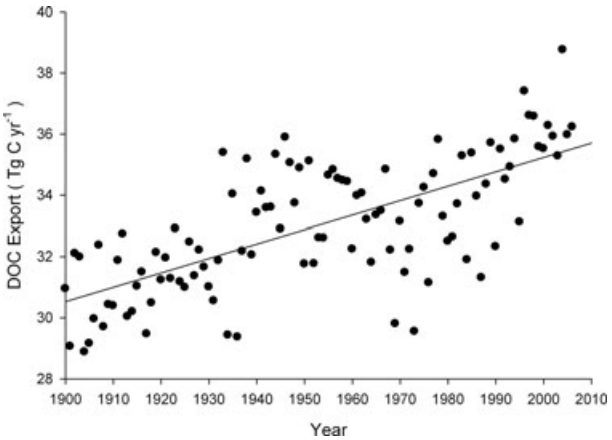

Fig. 12. TEM estimates of DOC export to the Arctic Ocean from surrounding watersheds between 1900 and 2006.

decomposition and hence produces more DOC. Thus, permafrost degradation accentuates the effects of warming on the DOC concentration of runoff.

Land-use change influences the availability of soil organic carbon in two ways in our simulations. First, the assumption of optimal fertilizer application of crops leads to carbon accumulation in agricultural soils in many regions in our simulations (see Felzer et al., 2004, 2005). Second, TEM assumes that a certain proportion of vegetation carbon is left behind as slash (McGuire et al., 2001) when natural areas are either converted to agriculture or when trees are harvested for timber. This slash is then added to the reactive soil organic carbon pool. The additional soil carbon resulting from either fertilizer applications or slash inputs increases DOC production by increasing the amount of reactive soil organic carbon that is available to decompose. In contrast, fires consume a portion of the soil organic matter (Balshi et al., 2007) so that there is less reactive soil organic carbon available to decompose and the production of DOC decreases.

The sensitivities described above suggest that the historical changes in microbial metabolism and land-use change have had a larger influence on changes in DOC export than fire. Thus, our 20th century results suggest that the delivery of DOC to the Arctic Ocean will likely increase as the climate warms.

4.5. *Sensitivity of ocean CO_2 fluxes*

In several studies on the Arctic Ocean, great emphasis has been given to the role of sea-ice cover in controlling the capability of the region to absorb atmospheric CO_2, both for the present climate and in the future if the dramatic reduction in sea-ice continues. It has been suggested by Bates et al. (2006) that the Arctic Ocean has increased its CO_2 sink mostly due to the progressive reduction in sea ice, especially during the summer when a more ice-free ocean would allow a larger CO_2 sink via increased biological production. However, it is possible that this enhanced production may be limited by nitrogen availability as reduced winter mixing and increased stratification from freshening may cause a reduction in nitrate concentrations in the surface layer (Lavoie et al., 2010).

From in situ biogeochemical measurements it has been estimated that from late 1970s to present that the sink strength of the Arctic Ocean CO_2 should have tripled from $\sim$20 to $\sim$66 Tg C yr^{-1} because of the trend of sea-ice reduction (Bates et al., 2006). Our estimate of mean ocean CO_2 uptake (57.8 Tg C yr^{-1}) is comparable to the estimate by Bates et al. (2006) and within the range of exchange (20–100 Tg C yr^{-1}) estimated by McGuire et al. (2009). However, it is on the lower end of the more recently published estimate that the Arctic Ocean CO_2 sink is currently between 65 and 175 Tg C yr^{-1} (Bates and Mathis, 2009).

Pabi et al. (2008) also estimated that the primary productivity of the Arctic Ocean increased over the time period 1998–2007 due to the progressive reduction of sea-ice cover. Furthermore, Arrigo et al. (2008) showed that in 2007 there was a notable lengthening of the growing season phytoplankton production in Arctic waters that was associated with the substantial reduction of sea-ice cover in that year. The results from these two studies based on remote sensing techniques indicate that interannual variability in Arctic sea-ice cover is the key driver that modulates the biological productivity of the Arctic Ocean. These findings are generally consistent with the results of our simulations, in which changes of the Arctic Ocean CO_2 sink are mostly driven by the progressive decline of sea-ice cover, although the interactions between sea-ice cover and SST fluctuations are also important. It is interesting to note that between 2004 and 2005 the estimated CO_2 sink of the Arctic Ocean in our simulations increased from $\sim$54 to $\sim$67 Tg C yr^{-1} in association with a dramatic reduction in sea-ice cover simulated by the sea-ice model; the simulated reduction is consistent with observations and also highlights the sensitivity of the ocean carbon cycle in the Arctic to the large variations of sea-ice cover.

The overall trend for the simulation period suggests that the dramatic reduction in sea-ice cover would enhance the strength of the biological pump, which promotes oceanic CO_2 uptake, although the progressive SST warming has an opposing effect since it lowers the efficiency of the solubility pump, which promotes CO_2 outgassing. During the recent decade of analysis, our simulations suggest that increased CO_2 uptake from the strengthening of the biological pump outpaced the increase in outgassing from the weakening of the solubility pump, resulting in an overall increasing trend in net CO_2 uptake by the Arctic Ocean. While the results of this study further suggest that the continued declines in sea ice cover will likely continue to strengthen the CO_2 sink of the ocean component of the Arctic Basin establishing a negative carbon-climate feedback in this particular area of the global ocean, an important uncertainty involves the effects of ocean acidification on the biological pump (Steinacher et al., 2009; Yamamoto-Kawai et al., 2009).

5. Conclusion

Our study indicates that between 1997 and 2006, the terrestrial regions of the Arctic were a source of carbon to the atmosphere and to the Arctic Ocean, and the Arctic Ocean was sequestering carbon from both the atmosphere and the land with the overall ocean sink greater than the land source by approximately 30 Tg C yr^{-1}. It is interesting to note that the magnitude of this sink is similar to the magnitude of the exchange of carbon as DOC between the land and the ocean in the Arctic. Because of CH_4 emissions of wetlands, the Arctic continues to act as source of green house gas forcing to the warming of the earth. Our analyses indicate that CH_4 emissions are increasing, and other studies have indicated that CH_4 emissions are expected to generally increase with continued warming of the Arctic (Gedney et al., 2004, Zhuang et al., 2006, 2007).

While both the lands and oceans of the Arctic were estimated to be sinks for atmospheric CO_2 between 1997 and 2006 in our study, it appears that the land sink is diminishing because of more fire disturbance in this decade compared to previous decades and the ocean sink is increasing because of increased biological pump activity associated with the reduction in sea ice cover. Our results suggest that the effects of fire in diminishing the CO_2 sink are currently stronger than the effects of reduced sea ice cover in enhancing the CO_2 sink. Continued warming of the Arctic is expected to substantially increase fire activity (Flannigan et al., 1998, Balshi et al., 2009) and reduce sea ice (ACIA 2004, 2005). Key research issues are to evaluate (1) whether the influence of continued warming on terrestrial processes affecting CO_2 exchange with the atmosphere will more than overwhelm the effects of reduced sea ice in enhancing CO_2 uptake by the Arctic Ocean and (2) whether the greenhouse gas forcing of CH_4 emissions will be enhanced or compensated by the response of CO_2 exchange to warming. The results of this study emphasize the importance of analysing the dynamics of the C balance in the Arctic as a linked system across the land–ocean–atmosphere domain in order to evaluate these questions. Earth system models that consider carbon-climate feedbacks should treat the carbon processes of the Arctic as a linked system.

6. Acknowledgments

We thank Eugenie Euskirchen, Fengming Yuan and an anonymous reviewer for comments on previous versions of this paper. This study was supported, in part, by the NSF Arctic System Science Program as part of the Arctic Carbon Cycle Synthesis Project (ARC-0531047, 0531082, 0531119 and 0554811).

References

ACIA. 2004. *Impacts of a Warming Arctic: Arctic Climate Impact Assessment–Synthesis Report*. Cambridge University Press, New York, NY, 45pp. Available at: http://amap.no/acia/.

ACIA. 2005. *Arctic Climate Impact Assessment–Scientific Report*. Cambridge University Press, New York, NY, 1042pp. Available at: http://amap.no/acia/.

Aitkenhead, J. A. and McDowell, W. H. 2000. Soil C:N ratio as a predictor of annual riverine DOC flux at local and global scales. *Global Biogeochem. Cycles* **14**, 127–138.

Arrigo, K., van Dijken, G. and Pabi, S. 2008. Impact of shriking Arctic ice cover on marine primary production. *Geophys. Res. Lett.* **35**, L19603.

Balshi, M. S., McGuire, A. D., Zhuang, Q., Melillo, J. M., Kicklighter, D. W. and co-authors. 2007. The role of historical fire disturbance in the carbon dynamics of the pan-boreal region: a process-based analysis. *J. Geophys. Res.–Biogeosci.* **112**, G02029. doi:10.1029/2006JG000380.

Balshi, M. S., McGuire, A. D., Duffy, P., Flannigan, M., Walsh, J. and co-authors. 2009. Assessing the response of area burned to changing climate in western boreal North America using a Multivariate Adaptive Regression Splines (MARS) approach. *Global Change Biol.* **15**, 578–600. doi:10.1111/j.1365-2486.2008.01679.x.

Bates, N. R. and Mathis, J. T. 2009. The Arctic Ocean marine carbon cycle: evaluation of air-sea CO_2 exchanges, ocean acidification impacts and potential feedbacks. *Biogeosci. Discuss.* **6**, 6695–6747.

Bates, N. R., Moran, S. D., Hansell, D. A. and Mathis, J. T. 2006. An increasing CO_2 sink in the Arctic Ocean due to the sea-ice loss. *Geophys. Res. Lett.* **33**, L23609. doi:10.1029/2006GL027028.

Beer, C., Lucht, W., Schmullius, C. and Shvidenko, A. 2006. Small net carbon dioxide uptake by Russian forests during 1981–1999. *Geophys. Res. Lett.* **33**, L15403. doi:10.1029/2006GL026919.

Carter, A. J. and Scholes, R. J. 2000. *Soil Data v2.0: Generating a Global Database of Soil Properties Report*. Environ. CSIR, Pretoria.

Chapin, F. S. III., McGuire, A. D., Randerson, J., Pielke, R., Sr., Baldocchi, D. and co-authors. 2000. Feedbacks from arctic and boreal ecosystems to climate. *Global Change Biol.* **6**, S211–S223.

Chapin, F. S., III, Berman, M., Callaghan, T., Ponvey, T., Crepin, A-S. and co-authors. 2005. Polar Systems. In: *The Millenium Ecosystem Assessment* (eds H. Hassan, R. Scholes and N. Ash), Island Press, Washington, DC, USA, 717–743.

Chapin, F. S., III, Woodwell, G. M., Randerson, J. T., Lovett, G. M., Rastetter, E. B. and co-authors. 2006. Reconciling carbon-cycle concepts, terminology, and methods. *Ecosystems* **9**, 1041–1050.

Chen, Y. -H. and Prinn, R. G. 2006. Estimation of atmospheric methane emissions between 1996 and 2001 using a three dimensional global chemical transport model. *J. Geophys. Res.* **111**, D10307. doi:10.1029/2005JD006058.

Clein, J. S., McGuire, A. D., Zhang, X., Kicklighter, D. W., Melillo, J. M. and co-authors. 2002. Historical and projected carbon balance of mature black spruce ecosystems across North America: the role of carbon-nitrogen interactions. *Plant Soil* **242**, 15–32.

Condron, A., Winsor, P., Hill, C. and Menemenlis, D. 2009. Response of the Arctic freshwater budget to extreme NAO forcing. *J. Clim.* **22**, 2422–2437.

Curry, J. A., Rossow, W. B., Randall, D. and Schramm, J. L. 1996. Overview of Arctic cloud and radiation conditions. *J. Clim.* **9**, 1731–1764.

Denman, K. L., Brasseur, G., Chidthaisong, A., Ciais, P., Cox, P. M. and co-authors. 2007. Couplings between changes in the climate system and biogeochemistry. In: *Climate Change 2007: The Physical Science Basis. Contribution of Working Group I to the Fourth Assessment Report of the Intergovernmental Panel on Climate Change* (eds S. Solomon, D. Qin, M. Manning, Z. Chen, M. Marquis and co-authors), Cambridge University Press, Cambridge, United Kingdom and New York, NY, USA, 499–587.

Drobot, S., Maslanik, J., Herzfeld, U. C., Fowler, C. and Wu, W. 2006. Uncertainty in temperature and precipitation datasets over terrestrial regions of the Western Arctic. *Earth Interact.* **10**, p. 23, 1–17.

Dutkiewicz, S., Sokolov, A., Scott, J. and Stone, P. 2005. A three-dimensional ocean-sea ice-carbon cycle model and its coupling to a two-dimensional atmospheric model: uses in climate change studies. In: *MIT Joint Program on Science and Policy of Global Change Report No. 122.* Massachusetts Institute of Technology, Cambridge, Massachusetts, 47.

Euskirchen, E. S., McGuire, A. D., Kicklighter, D. W., Zhuang, Q., Clein, J. S. and co-authors. 2006. Importance of recent shifts in soil

thermal dynamics on growing season length, productivity and carbon sequestration in terrestrial high-latitude ecosystems. *Global Change Biol.* **12**, 731–750.

Euskirchen, S. E., McGuire, A. D. and Chapin, F. S., III. 2007. Energy feedbacks of northern high-latitude ecosystems to the climate system due to reduced snow cover during 20th Century warming. *Global Change Biol.* **13**, 2425–2438.

Felzer, B., Kicklighter, D., Melillo, J., Wang, C., Zhuang, Q. and co-authors. 2004. Effects of ozone on net primary production and carbon sequestration in the conterminous United States using a biogeochemistry model. *Tellus* **56B**, 230–248.

Felzer, B., Reilly, J., Melillo, J., Kicklighter, D., Sarofim, M. and co-authors. 2005. Future effects of ozone on carbon sequestration and climate change policy using a global biogeochemical model. *Clim. Change* **73**, 345–373. doi:10.1007/s10584-005-6776-4.

Flannigan, M. D., Bergeron, Y., Engelmark, O. and Wotton, B. M. 1998. Future wildfire in circumboreal forests in relation to global warming. *J. Vegetat. Sci.* **9**, 469–476.

French, N. H. F., Kasischke, E. S. and Williams, D. G. 2002. Variability in the emission of carbon-based trace gases from wildfire in the Alaskan boreal forest. *J. Geophys. Res.* **107**, 8151. doi:10.1029/2001JD000480.

Gedney, N., Cox, P. M. and Huntingford, C. 2004. Climate feedback from wetland methane emissions. *Geophys. Res. Lett.* **31**, L20503. doi:10.1029/2004GL020919.

Goetz, S. J., Bunn, A. G., Fiske, G. J. and Houghton, R. A. 2005. Satellite-observed photosynthetic trends across boreal North America associated with climate and fire disturbance. *Proc. Natl. Acad. Sci.* **102**, 13521–13525.

Goetz, S. J., Mack, M. C., Gurney, K. R., Randerson, J. T. and Houghton, R. A. 2007. Ecosystem responses to recent climate change and fire disturbance at northern high latitudes: observations and model results contrasting northern Eurasia and North America. *Environ. Res. Lett.* **2**, 045031. doi:10.1088/1748-9326/2/4/045031.

Gurney, K. R., Law, R. M., Denning, A. S., Rayner, P. J., Baker, D. and co-authors. 2002. Towards robust regional estimates of CO_2 sources and sinks using atmospheric transport models. *Nature* **415**, 626–630. doi:10.1038/415626a.

Gurney, K. R., Law, R. M., Denning, A. S., Rayner, P. J., Pak, B. C. and co-authors. 2004. Transcom 3 inversion intercomparison: model mean results for the estimation of seasonal carbon sources and sinks, Global Biogeochem. *Cycles* **18**, GB1010. doi:10.1029/2003GB002111.

Gurney, K. R., Baker, D., Rayner, P. and Denning, S. 2008. Interannual variations in continental-scale net carbon exchange and sensitivity to observing networks estimated from atmospheric CO_2 inversions for the period 1980 to 2005. *Global Biogeochem. Cycles* **22**, GB3025. doi:10.1029/2007GB003082.

Hinzman, L. D., Bettez, N. D., Bolton, W. R., Chapin, F. S., Dyurgerov, M. B. and co-authors. 2005. Evidence and implications of recent climate change in northern Alaska and other Arctic regions. *Clim. Change* **72**, 251–298.

Hurtt G. C., Frolking, S., Fearon, M. G., Moore, B., Shevliakova, E. and co-authors. 2006. The underpinnings of land-use history: three centuries of global gridded land-use transitions, wood harvest activity, and resulting secondary lands. *Global Change Biol.* **12**, 1208–1229. doi:10.1111/j.1365-2486.2006.01150.x.

IPCC. 2007. Climate change 2007: the physical science basis. In: *Contribution of Working Group I to the Fourth Assessment Report of the Intergovernmental Panel on Climate Change* (eds S. Solomon, D. Qin, M. Manning, Z. Chen, M. Marquis and co-authors), Cambridge University Press, Cambridge, United Kingdom and New York, USA, 996.

Jain, A., Yang, X., Kheshgi, H., McGuire, A. D., Post, W. and co-authors. 2009. Nitrogen attenuation of terrestrial carbon cycle response to global environmental factors. *Global Biogeochem. Cycles* **23**, GB4028. 13 pp., doi:10.10292009GB003519.

Kalnay, E., Kanamitsu, M., Kistler, R., Collins, W., Deaven, D. and co-authors. 1996. The NCEP/NCAR 40-year reanalysis project. *Bull. Am. Meteorol. Soc.* **77**, 437–471.

Kasischke, E. S. and Bruhwiler, L. P. 2003. Emissions of carbon dioxide, carbon monoxide, and methane from boreal forest fires in 1998. *J. Geophys. Res.* **108**, D18146. doi:10.10292001JD000461.

Keeling, C. D. and Whorf, T. P. 2005. *Atmospheric CO_2 Records from Sites in the SIO Air Sampling Network*. Carbon Dioxide Information Analysis Center, Oak Ridge, TN.

Kicklighter, D. W., Bruno, M., Dönges, S., Esser, G., Heimann, M. and co-authors. 1999. A first-order analysis of the potential role of CO_2 fertilization to affect the global carbon budget: a comparison study of four terrestrial biosphere models. *Tellus* **51B**, 343–366.

Lammers, R. B., Shiklomanov, A. I., Vörösmarty, C. J., Fekete, B. M. and Peterson, B. J. 2001. Assessment of contemporary Arctic river runoff based on observational discharge records. *J. Geophys. Res.* **106**, 3321–3334.

Lavoie, D., Denman, K. L. and Macdonald, R. W. 2010. Effects of future climate change on primary productivity and export fluxes in the Beaufort Sea. *J. Geophys. Res.-Oceans* **115**, C04018. doi:10.1029/2009JC005493.

Lenton, T. M., Held H., Kriegler, E., Hall, J. W., Lucht, W. and co-authors. 2008. Tipping elements in the earth's climate system. *Proc. Natl. Acad. Sci. U.S.A.* **105**, 1786–1793. doi:10.1073/pnas.0705414105.

Loveland, T. R., Reed, B. C. Brown, J. F., Ohlen, D. O., Zhu, Z. and co-authors. 2000. Development of a global land cover characteristics database and IGBP DISCover from 1 km AVHRR data. *Int. J. Remote Sens.* **21**, 1303–1330.

MacLean, R., Oswood, M. W., Irons, J. G., III and McDowell, W. H. 1999. The effect of permafrost on stream biogeochemistry: a case study of two streams in the Alaskan (U.S.A) taiga. *Biogeochemistry* **47**, 239–267.

Manizza, M., Follows, M. J., Dutkiewicz, S., McClelland, J. W., Menemenlis, D. and co-authors. 2009. Modeling transport and fate of riverine dissolved organic carbon in the Arctic Ocean. *Global Biogeochem. Cycles* **23**, GB4006. doi:10.1029/2008GNB003396.

Marshall, J., Hill, C., Perelman, L. and Adcroft, A. 1997. Hydrostatic, quasi-hydrostatic and nonhydrostatic ocean modeling. *J. Geophys. Res.* **102**(C3), 5733–5752.

Matthews, E. and Fung, I. 1987. Methane emissions from natural wetlands: global distribution, area, and environmental characteristics of sources. *Global Biogeochem. Cycles* **1**, 61– 86.

McClelland, J. W., Holmes, R. M., Peterson, B. J., Amon, R., Brabets, T. and co-authors. 2008. Development of a pan-Arctic database for river chemistry. *EOS* **89**. doi:10.1029/2008EO240.001.

McGuire, A. D., Melillo, J. M., Joyce, L. A., Kicklighter, D. W., Grace, A. L. and co-authors. 1992. Interactions between carbon and nitrogen dynamics in estimating net primary productivity for potential vegetation in North America. *Global Biogeochem. Cycles* **6**, 101–124.

McGuire, A. D., Melillo, J. M., Kicklighter, D. W., Pan, Y., Xiao, X. and co-authors. 1997. Equilibrium responses of global net primary production and carbon storage to doubled atmospheric carbon dioxide: sensitivity to changes in vegetation nitrogen concentration. *Global Biogeochem. Cycles* **11**, 173–189.

McGuire, A.D., Sitch, S., Clein, J. S., Dargaville, R., Esser, G. and co-authors. 2001. Carbon balance of the terrestrial biosphere in the twentieth century: analyses of CO_2, climate and land-use effects with four process-based ecosystem models. *Global Biogeochem. Cycles* **15**, 183–206.

McGuire, A. D., Chapin, F. S., III, Walsh, J. E. and Wirth, C. 2006. Integrated regional changes in arctic climate feedbacks: implications for the global climate system. *Ann. Rev. Environ. Resour.* **31**, 61–91.

McGuire, A. D., Anderson, L. G., Christensen, T. R., Dallimore, S., Guo, L. and co-authors. 2009. Sensitivity of the carbon cycle in the Arctic to climate change. *Ecol. Monogr.* **79**, 523–555.

Menemenlis, D., Hill, C., Adcroft, A., Campin, J., Cheng, B. and co-authors. 2005. NASA Supercomputer Improves Prospects for Ocean Climate Research. *EOS* **86**, 89.

Mitchell, T. D. and Jones, P. D. 2005. An improved method of constructing a database of monthly climate observations and associated high-resolution grids. *Int. J. Climatol.* **25**, 693–712.

Myneni, R. B., Keeling, C. D., Tucker, C. J., Asrar, G. and Nemani, R. R. 1997. Increased plant growth in the northern high latitudes from 1981–1991. *Nature* **386**, 698–701.

Myneni, R. B., Dong, J., Tucker, C. J., Kaufmann, R. K., Kauppi, P. E. and co-authors. 2001. A large carbon sink in the woody biomass of northern forests. *Proc. Natl. Acad. Sci. USA* **98**, 14784–14789.

Pabi, S., G. van Dijken, L. and Arrigo, K. 2008. Primary production in the Arctic Ocean, 1998–2006. *J. Geophys. Res.–Oceans* **113**, C08005. doi:10.1029/2007JC004578.

Pacala, S., Birdsey, R. A., Bridgham, S. D., Conant, R. T., Davis, K. and co-authors. 2007. The North American Carbon Budget Past and Present. In: *The First State of the Carbon Cycle Report (SOCCR): The North American Carbon Budget and Implications for the Global Carbon Cycle. A Report by the U.S. Climate Change Science Program and the Subcommittee on Global Change Research* (eds A. W. King, L. Dilling, G. P. Zimmerman, D. M. Fairman, R. A. Houghton and co-editors), National Oceanic and Atmospheric Administration, National Climatic Data Center, Asheville, NC, USA, 29–36.

Peterson, B. J., Hobbie, J. E. and Corliss, T. L. 1986. Carbon flow in a tundra stream ecosystem. *Can. J. Fisher. Aquat. Sci.* **43**, 1259–1270.

Petrone, K. C. 2005. *Export of Carbon Nitrogen and Major Solutes from a Boreal Forest Watershed: The Influence of Fire and Permafrost*. PhD. Dissertation. University of Alaska Fairbanks, 132.

Polyakov, I. D., Alekseev, G. V., Bekryaev, R. V., Bhatt, U., Colony, R. and co-authors. 2002. Observationally based assessment of polar amplification of global warming. *Geophys. Res. Lett.* **29**, 1878. doi:10.1029/2001GL011111.

Post, E., Forchhammer, M. C., Bret-Harte, M. S., Callaghan, T. V., Christensen, T. R. and co-authors. 2009. Ecological dynamics across the arctic associated with recent climate change. *Science* **325**, 1355–1358. doi:10.1126/science.1173113.

Raich, J. W., Rastetter, E. B., Melillo, J. M., Kicklighter, D. W., Steudler, P. A. and co-authors. 1991. Potential net primary productivity in South America: application of a global model. *Ecol. Appl.* **1**, 399–429.

Raymond, P. A., McClelland, J., Holmes, R., Zhulidov, A., Mull, K. and co-authors. 2007. Flux and age of dissolved organic carbon exported to the arctic ocean: a carbon isotopic study of the five largest arctic rivers. *Global Biogeochem. Cycles* **21**, GB4011. doi:10.1029/2007GB002.934.

Sarmiento, J. L. and Gruber, N. 2006. *Ocean Biogeochemical Dynamics*. Princeton University Press, Princeton, USA.

Schuur, E. A. G., Vogel, J. G., Crummer, K. G., Lee, H., Sickman, J. O. and co-authors. 2009. The effect of permafrost thaw on old carbon release and net carbon exchange from tundra. *Nature* **459**, 556–559.

Serreze, M. C. and Francis, J. A. 2006. The Arctic amplification debate. *Clim. Change* **76**, 241–264.

Serreze, M. C., Walsh, J. E., Chapin, F. S., III, Osterkamp, T., Dyurgerov, M. and co-authors. 2000. Observational evidence of recent change in the northern high-latitude environment. *Clim. Change* **46**, 159–207.

Shiklomanov, I., Shiklomanov, A., Lammers, R., Peterson, B., and Vorosmarty, C. 2000. The Dynamics of River Water Inflow to the Arctic Ocean. In: *The Freshwater Budget of the Arctic Ocean* (ed. E. Lewis). Kluwer Academic Press, 281–296.

Sokolov, A. P., Kicklighter, D. W., Melillo, J. M., Felzer, B. S., Schlosser, C. A. and co-authors. 2008. Consequences of considering carbon-nitrogen interactions on the feedbacks between climate and the terrestrial carbon cycle. *J. Clim.* **21**, 3776–3796. doi:10.1175/2008JCLI2038.1.

Steinacher, M., Joos, F., Frölicher, T. L., Plattner, G.-K. and Doney, S. C. 2009. Imminent ocean acidification in the Arctic projected with the NCAR global coupled carbon cycle-climate model. *Biogeosciences* **6**, 515–533.

Stroeve, J., Holland, M. M., Meier, W., Scambos, T. and Serreze, M. 2007. Arctic sea ice decline: faster than forecast. *Geophys. Res. Lett.* **34**, L09501. doi:10.1029/2007GL029703.

Thornton, P. E., Lamarque, J.-F., Rosenbloom, N. A. and Mahowald, N. M. 2007. Influence of carbon-nitrogen cycle coupling on land model response to CO_2 fertilization and climate variability. *Global Biogeochem. Cycles* **21**, GB4018. doi:10.1029/2006GB002868.

Van Der Werf, G. R., Randerson, J. T., Giglio, L., Collatz, G. J., Kasibhatla, P. S. and co-authors. 2006. Interannual variability in global biomass burning emissions from 1997 to 2004. *Atmos. Chem. Phys.* **6**, 3423–3441.

van Drecht, G., Bouwman, A. F., Knoop, J. M., Beusen, A. H. W., and Meinardi, C. R. 2003. Global modeling of the fate of nitrogen from point and nonpoint sources in soils, groundwater, and surface water. *Global Biogeochem. Cycles* **17**, 1115. doi:10.1029/2003GB002060.

Xiao, X., Kicklighter, D. W., Melillo, J. M., McGuire, A. D., Stone P. H. and co-authors. 1997. Linking a global terrestrial biogeochemical model and a 2-dimensional climate model: implications for the carbon budget. *Tellus* **49B**, 18–37.

Yamamoto-Kawai, M., McLaughlin, F. A., Carmack, E. C., Nishino, S. and Shimada, K. 2009. Aragonite undersaturation in the Arctic Ocean: effects of ocean acidification and sea ice melt. *Science* **326**, 1098–1100.

Zhuang, Q., McGuire, A. D., Melillo, J. M., Clein, J. S., Dargaville, R. J. and co-authors. 2003. Carbon cycling in extratropical terrestrial

ecosystems of the Northern Hemisphere during the 20th Century: a modeling analysis of the influences of soil thermal dynamics. *Tellus* **55B**, 751–776.

Zhuang, Q., Melillo, J. M., Kicklighter, D. W., Prinn, R. G., McGuire, A. D. and co-authors. 2004. Methane fluxes between terrestrial ecosystems and the atmosphere at northern high latitudes during the past century: a retrospective analysis with a process-based biogeochemistry model. *Global Biogeochem. Cycles* **18**, GB3010. doi:10.10292004GB002239.

Zhuang, Q., Melillo, J. M., Sarofim, M. C., Kicklighter, D. W., McGuire, A. D. and co-authors. 2006. CO_2 and CH_4 exchanges between land ecosystems and the atmosphere in northern high latitudes over the 21st century. *Geophys. Res. Lett.* **33**, L17403. doi:10.1029/2006GL026972.

Zhuang, Q., Melillo, J. M., McGuire, A. D., Kicklighter, D. W., Prinn, R. G. and co-authors. 2007. Net emissions of CH_4 and CO_2 in Alaska: implications for the region's greenhouse gas budget. *Ecol. Appl.* **17**, 203–212.